

ResearchOnline@JCU

This file is part of the following reference:

Grabovickic, Stephanie (2000) *Petrology and structure of high-grade calcsilicates and granites of the Inkerman Shear Zone*. PhD thesis, James Cook University.

Access to this file is available from:

<http://eprints.jcu.edu.au/28253/>

If you believe that this work constitutes a copyright infringement, please contact ResearchOnline@jcu.edu.au and quote <http://eprints.jcu.edu.au/28253/>

Petrology and Structure of High-grade Calcsilicates and Granites of the Inkerman Shear Zone

**Thesis submitted by
Stephanie Grabovickic Bsc (Hons)
In December 2000**

**Dissertation submitted in partial fulfillment of the requirement for the degree of
Master of Science (Exploration and Mining) in the School of Earth Science at
James Cook University of North Queensland**

ABSTRACT

The Inkerman Shear Zone represents a characteristic structurally anomalous series of lineaments with a west – southwest trend. Low outcropping ridges of amphibolites, calcsilicates and granitic gneiss that form an older metamorphic unit represent these lineaments. Permo-Carboniferous dykes of various compositions form a dominant structural trend at right angles to these ridges. It is strictly not a shear zone of Permo-Carboniferous age, but represents a high strain zone of amphibolite facies metamorphics and granitoids (Inkerman Metamorphics).

The metamorphic rocks have undergone different metasomatic changes including the skarn development within the lithologies of the study area. Amphibolite found in the area generally is strongly foliated hornblende-plagioclase-quartz rock with accessory magnetite and titanite. Various calcsilicate rocks are common and are usually medium to coarse grained. In composition they vary from wollastonite-garnet rocks to various layered gneisses composed of garnet, clinopyroxene, hornblende, plagioclase and quartz.

The most common foliation fabric that can be found in the Inkerman Metamorphics has been named S_2 . This fabric has developed during the second deformation event D_2 that was marked by intrusion of abundant granitic veins. A large body of monzogranite found in the southern part of the study area have a weak steeply dipping S_2 or S_4 foliation. Therefore, the granitoids of the study area are intruded pre D_4 or alternatively intruded late in D_2 .

The peak metamorphic conditions were obtained at 4.5 kbar, at temperatures up to 650° C and at low X_{CO_2} conditions. Inclusions in garnet porphyroblasts in Ink2 indicate several growth stages, with S_2 developed in the matrix only, so the earlier metamorphic growth stages occurred under static conditions. This was calculated using a pressure determined from Hornblende on a granodiorite

vein and a phase diagram calculated using "Thermocalc" for assemblages in sample Ink2.

Because of local metasomatism, many granitic veins contain clinopyroxene and anorthite rich plagioclase, up to An₉₀, it is postulated that the metasomatic conditions resulted in the conversion of granitic veins to endoskarn. This metasomatic process involved addition of Ca and probable removal of alkalis (Na and K). Consequently, most of the endoskarn veins are composed of Ca rich plagioclase and with very little or no K-feldspar. These pegmatitic veins are probably late D₂ to post D₂. Small pods of andradite-rich garnet formed earlier were boudinaged during D₂.

Ages of the deformation events related to the formation of the Inkerman Metamorphics are uncertain. Correlatives may be found in metamorphic rocks of Argentina and Running River Metamorphics and are likely to be Proterozoic to Lower Palaeozoic. The peak metamorphism of the Harvey's Range rocks was syn-D₃. Foliation S₃ (Edison, 1995.) that corresponds to this event is of similar orientation to S₂ foliation found in the Inkerman Metamorphics.

Declaration

I declare that this thesis is my own work and has not been submitted in any form for another degree or diploma at any university or other institution of tertiary education. Information derived from the published or unpublished work of others has been acknowledged in the text and a list of references is given.

Stephanie Grabovickic

20 December 2000.

Statement of Access

I, the undersigned, the author of this thesis, understand that James Cook University of North Queensland will make available for use within the University Library and, by microfilm or other means, allow access to users in other approved libraries. All users consulting this thesis will have to sign the following statement:

In consulting this thesis I agree not to copy or closely paraphrase it in whole or in part without the written consent of the author, and to make proper public written acknowledgement for any assistance that I have obtained from it.

Beyond this, I do not wish to place any restrictions on access to this thesis.

Stephanie Grabovickic

20 December 2000.

Acknowledgements

The author would like to acknowledge the support, assistance and help of the following listed people:

My special thanks to my supervisor Dr Mike Rubenach for his continued help during the field and research part of the thesis.

Special thanks to Damien Foster, PhD student at James Cook University Townsville for his help with the thin sections and general suggestions related to the study area.

I am grateful to my good friends Mary Wallace, Debbie Lethbridge and Dave Jenkins for their editing assistance. Special thanks to Rob Lewis for his help with map drafting. Terra Search is thanked for the permission to use drafting equipment.

And to all those that supported me during all these years but I forgot to mention. Thanks.

Table of Contents

Abstract	ii
Declaration	iv
Statement of Access	v
Acknowledgements	vi
Table of Contents	vii
List of Figures	viii
List of Tables	x
Chapter One: Introduction	
1.1. General Introduction	1
1.2. Aims	1
1.3. Location, Access and Vegetation	1
1.4. Scope of Study	4
1.5. Previous Work	5
Chapter Two: Regional Geology	
2.1. Regional Geology	7
2.2. Correlation and Origin of Metamorphic Rocks	10
Chapter Three: Local Geology	
3.1. Introduction	12
3.2. Metamorphic Unit	12
3.2.1. amphibolite	12
3.2.2. calcsilicate rocks	14
3.2.3. granitoid gneiss	16
3.3. The Intrusive Rock Unit	18
3.3.1. granitoid veins	18
3.3.2. leucocratic syenogranite	18
3.3.3. mafic dykes	20
Chapter Four: Structural Geology	
4.1. Introduction	22
4.2. Second Deformation Event (D ₂)	22
4.3. Third Deformation Event (D ₃)	25
4.4. Fourth Deformation Event (D ₄)	27
4.5. Other Structural Characteristics	27
Chapter Five: Petrology and Mineral Chemistry	
5.1. Introduction	30
5.2. Calcsilicate Assemblages	31
5.2.1. calcsilicate rock with wollastonite, garnet, vesuvianite, diopside and calcite	32
5.2.2. calcsilicate rock with quartz, plagioclase, pyroxene and epidote	35
5.2.3. other calcsilicates	40
5.3. Amphibolite	43
5.4. Leuco Granite	44

5.5. Phase Diagram	45
Chapter Six: Discussion and Conclusions	
6.1. Introduction	48
6.2. Geological History	49
6.3. Origin of the Calcsilicates and Skarns	49
6.3.1. calcsilicate reactions	50
6.3.2. skarn formation	50
6.4. Future Work	51
References	52

Appendices

Appendix 1: Microprobe Analysis	54
Appendix 2: Thin Sections	65
Appendix 3 Sample List and Catalogue Number	79

List of Figures

Figure 1.1.	A photo of the project area partly showing a coastline	2
Figure 1.2.	Location Map	3
Figure 2.1.	Geological Provinces and Subprovinces of NE Qld	9
Figure 3.1.	Field photograph of banded calcsilicate	14
Figure 3.2.	Field photograph of banded calcsilicate outcrop	15
Figure 3.3.	Field photograph of calcsilicate outcrop	16
Figure 3.4.	Field photograph of granitic gneiss	17
Figure 3.5.	Field photograph of a pink syenogranite outcrop	19
Figure 3.6.	Field photograph of a mafic dyke	20
Figure 4.1.	Field photograph of banded calcsilicate showing foliation	23
Figure 4.2.	Field photograph of calcsilicate with a pegmatitic vein	24
Figure 4.3.	Field photograph of calcsilicate with folds and foliation	24
Figure 4.4.	Field photograph of calcsilicate with F_2 and F_3	25
Figure 4.5.	Field photograph of folded calcsilicate	26
Figure 4.6.	Photograph of a oriented calcsilicate specimen	28
Figure 4.7.	Inkerman Shear Zone, Geology, Structure and Sample Location	29
Figure 5.1.	Photomicrograph of Ink2	34
Figure 5.2.	Photomicrograph of Ink2	34
Figure 5.3.	Photomicrograph of Ink11	35
Figure 5.4.	Photomicrograph of Ink12	36
Figure 5.5.	Photomicrograph of HH7	37
Figure 5.6.	Photomicrograph of HH4	38
Figure 5.7.	Photomicrograph of HHA9	38
Figure 5.8.	Photomicrograph of Ink12	39
Figure 5.9.	Photomicrograph of H3	41
Figure 5.10.	Photomicrograph of HHA7	41
Figure 5.11.	Photomicrograph of HHA12	42
Figure 5.12.	Photomicrograph of Ink8	42
Figure 5.13.	Photomicrograph of Ink7	43
Figure 5.14.	Photomicrograph of Ink6	44
Figure 5.15.	Phase Diagram: T – X_{CO_2} plot	47

Chapter One

Introduction

1.1. General Introduction

A portion of the “Inkerman Shear Zone” that is located on the southern bank of the Burdekin River, southwest of Home Hill was the subject of this study. The project involved a detailed study of two suites of lithologies that are interpreted to be of very different age. Amphibolites, various calcsilicates rocks and granitoid gneiss form an older unit. The younger sequence is represented by a group of different granitoids and syenogranites. Permo-Carboniferous mafic dykes postdate these two lithological units.

Through the detailed field mapping and laboratory examination of the thin sections microstructural characteristics and the mineral assemblages of the lithological units were defined and presented in this thesis.

1.2. Aims

Aims of the thesis are to establish structural characteristics, metamorphism and geological history of the area.

1.3. Location, Access and Vegetation

The locality studied forms a small part of the Inkerman Shear Zone and is located approximately 140 km south of Townsville and approximately 15 to 20 km southwest of the town of Home Hill, on the southern bank of the Burdekin River. It lies on the Ayr 1:100,000 map, sheet no. 8358, and covers portions of Inkerman and Leichhardt Downs properties.

Access to the study area is via the Bruce Highway to Inkerman Station and then west via track to the homestead. The homestead belongs to the Cox family.



Figure 1.1. A photo of the project area partly showing a costean, looking southeast. The main rock in the costean is amphibolite and at the very far south end of the costean contact with granite is visible.

The terrain that surrounds the study area is flat to gently rolling cattle country, with only a couple of small hills. One of the hills is part of the study area and belongs to an eastern offshoot of Stokes Range within the Inkerman Shear Zone. This area forms a prominent ridgeline, approximately 5km long, with the maximum elevation of 122m.

Natural savannah woodland dominates the vegetation. The area is sparsely vegetated with low trees that commonly line creeks. During the period 1997-98, when mapping was completed, the area was largely covered with grass. Outcrop is generally good.

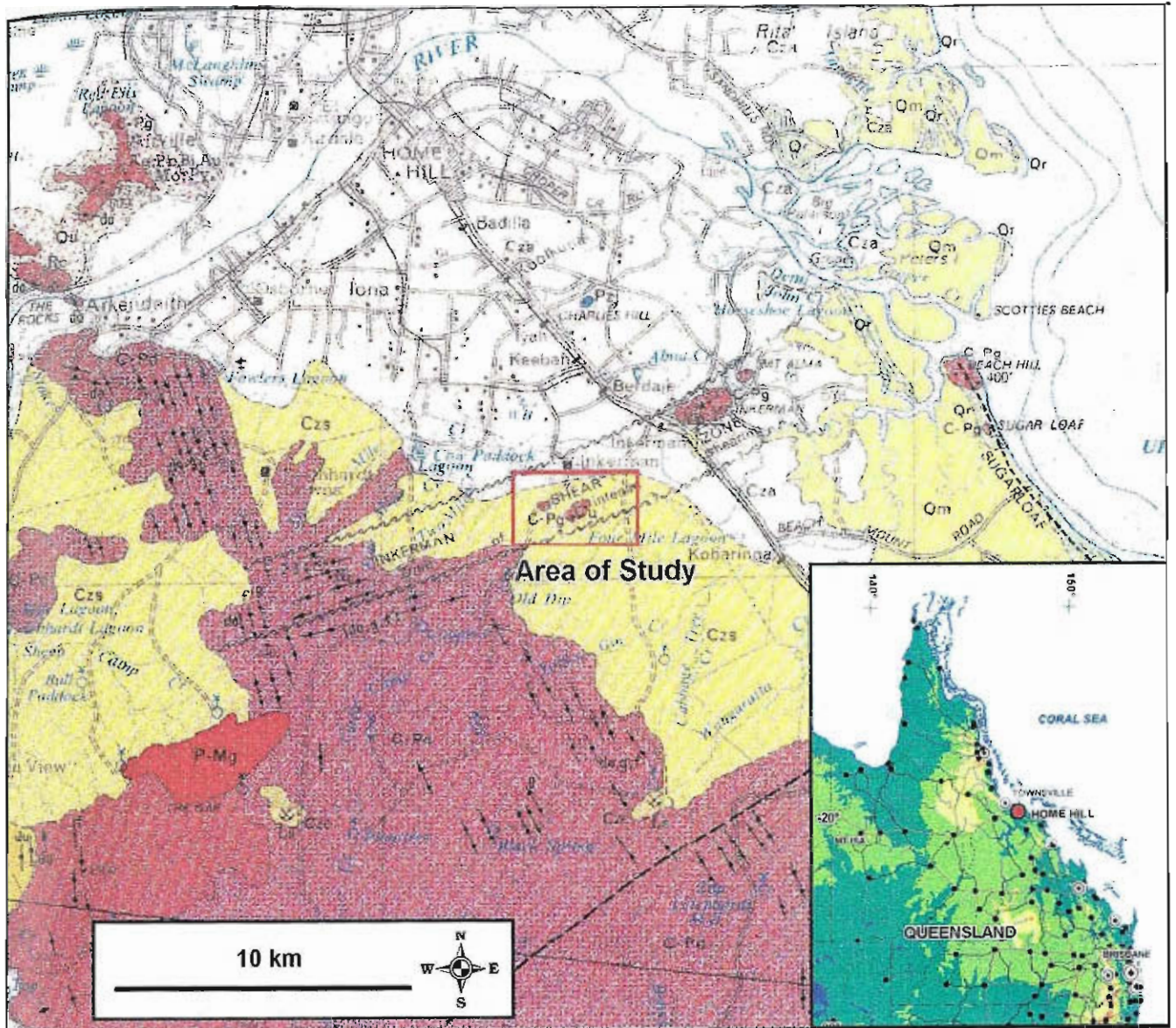


Figure 1.2. Location Map, taken from 1:250,000 geological sheet Ayr where wide Inkerman Shear Zone was mapped by A.G.L. Paine and C.M. Gregory (1969). It was taught that wide spread Upper Carboniferous to Lower Permian granite, adamellite, diorite and tonalite have been sheared and recrystallised as gneiss and in some places skarn-like rocks have been formed by metasomatism of these plutonic rocks and dykes.

1.4. Scope of the Study

The current project entailed a detailed study of a range of different lithologies from the area that is known as the Inkerman Shear Zone. The detailed mapping of the area (6 days) took place during the summer 1997, when the mapped area was divided into lithological units and samples were collected for thin and polished sections. Through the detailed laboratory examination of the thin sections, the mineral assemblage and microstructural characteristics of the lithological units were defined and are presented in this thesis. Selected polished sections were analysed by the electron microprobe at the JCU microprobe laboratory.

A phase diagram is presented showing the detailed relationships between different mineral assemblages and lithologies from the mapped area. "Thermocalc" was used to calculate the stability of important phases, relative to XCO_2 and temperature of the metamorphism.

A geological map of the area was also compiled showing the lithological and structural details for the mapped area.

1.5. Previous Work

The Commonwealth Scientific and Industrial Research Organizations (CSIRO) Division of Land Research and Regional Survey did the earliest work carried out in this area during the survey of the Townsville-Bowen region. This survey included the Ayr sheet and was conducted during 1950-1951. The area of Stokes Range had been mapped as late Devonian volcanics, which had been intruded by northwest trending dykes of diorite composition (Traves, 1951). At the same time the granitoids in the adjacent area were mapped of possible Permian age.

In 1965 the Bureau of Mineral resources (BMR) carried out a regional geochemical survey of the 1:250,000 Ayr sheet area. The area was revised by Paine et al. (1970) and Gregory (1969), when it was suggested that the majority of the rock in the area south of Home Hill, the Stokes Range area, consists of late Carboniferous to early Permian granitoids. These were intruded by dykes, which differ in age, lithology, and orientation. The dominant, north-east trending structure was recognised and named as the Inkerman Shear Zone. Coarse-grained plutonic rocks, most likely granitoids that were sheared, hydrothermally altered and deformed giving a gneissic texture, represented the shear zone.

The work of Carruthers, 'Vermiculite and Asbestos Occurrences Home Hill District' (1954) suggested that the rocks at Six Mile Creek and in Stokes Range belong to the same series.

In the period of late 1960's and early 1970's Trans Australian Explorations Pty Ltd conducted an exploration program over the area on the eastern part of Stokes Range. The program consisted of stream sediment geochemistry, geological mapping, rock chip sampling and a magnetic survey. Nisbet and Goulevich (Company Report 3342, 1970) concluded that the rocks in the prospect area are a metamorphic sequence of uncertain age. These rocks are

intruded by three main phases of igneous rocks. Consequently, it was suggested that the Inkerman Shear Zone might represent an area of metamorphic basement rocks and not a shear zone as was suggested by Paine et al. (1970).

During the 1980's this area was a subject of a hydrological investigation by the Water Resources Commission. The investigation included geological traverses, geophysics and intensive drilling and hydro geological testing. A new unit, the Inkerman Metamorphics, was defined by Evans (1988, in Evans 1991). These consist of strongly foliated and layered rocks, metamorphosed to amphibolite grade. This unit was found inside and outside of the area previously mapped as the Inkerman Shear Zone. The presence of highly metamorphosed rocks contradicted the regional mapping of Paine et al. (1970) who suggested that the foliated and layered rocks belonged to the sequence of altered granitoids. The new interpretation was supported by the petrographic examination of Davies (1983, in Evans 1991) who suggested that the highly sheared amphibolite probably belongs to the basement rocks that were intruded by igneous rocks of varying composition.

In 1994 a small field project was conducted by D. Foster, which included structural mapping for 2 km along one of the prominent ridges on the eastern offshoot of Stokes Range. Foster concluded that the lithologies present include carbonate rich sediments and intrusive granitoids and show a complex deformation and metamorphism history. Some of the photos and thin sections taken by Foster were used in this project.

Chapter Two

Regional Geology

2.1. Regional Geology

The area mapped as the Inkerman Shear Zone is located in the Permian-Carboniferous Coastal Ranges Igneous Province and on the eastern edge of the Lolworth-Ravenswood Block. In the south the rocks of the late Paleozoic Bowen and Drummond Basin bound the area.

The Charters Towers Province is composed of the Running River, Argentine, Charters Towers and Cape River Metamorphics along with the Ravenswood and Lolworth Batholiths and the Falls Creek Tonalite. (Fig. 2.1.)

The Cape River Sub-province forms the basement in the Charter Towers Province and includes the Cape River Metamorphics in the western part of the region. The Charters Towers Metamorphics occupy the central part, and the Running River and Argentine Metamorphics are found in the northern part of the region. The Cape River Metamorphics are probably Neoproterozoic or Early Cambrian as was suggested by Withnall and Hutton (1991, in Hutton et al., 1995).

The Charters Towers Metamorphics include meta-pelitic schists, quartzite and calc-silicate rocks that have been intruded by mafic and felsite-pegmatite dykes and microdiorite. Although the age of the Charters Towers Metamorphics is unknown they are included in the Cape River Province as they have similar lithological and structural characteristics. Mid Ordovician, probably S-type

granites are associated with middle to upper amphibolite grade metamorphism in the Charters Towers and Argentine Metamorphics (Withnall et al. 1995).

The Argentine Metamorphics are composed of two packages: a lower grade package consists predominantly of mica schist and quartzite with minor intervals of laminated amphibolite, chlorite schist, calc-silicate rocks and impure marble. The high-grade package consists of migmatite biotite gneiss and mica schist of middle to upper amphibolite facies. The relationship between the high grade to lower grade packages is uncertain. Withnall & McLennan (1991) (1995) noted that in some places the boundary appears to be transitional as opposed to the suggestion of Hammond (1986) interpreted the contact as a major detachment zone between rocks of different ages. The Running River Metamorphics are similar to the high-grade package of the Argentine Metamorphics but are dominated by amphibolite and migmatite.

Rocks in the Lolworth-Ravenswood Province could have potential correlatives in the rocks of the Anakie Metamorphic Group, which were metamorphosed and deformed in the late Cambrian Delamerian Orogeny. For instance, the Argentine Metamorphic are similar in structure and lithology to the rocks of the Anakie Metamorphic Group (Withnall & McLennan, 1991). In particular, the Argentine Metamorphics have similar lithological and structural characteristics to the Anakie Metamorphics with the main fabric described as mylonitic, shallow dipping and probably initially flat laying.

Rocks of the Inkerman Shear Zone may represent an area of metamorphic basement rocks as many similar rocks can be found in the Anakie Metamorphics and also in the Argentine Metamorphics.

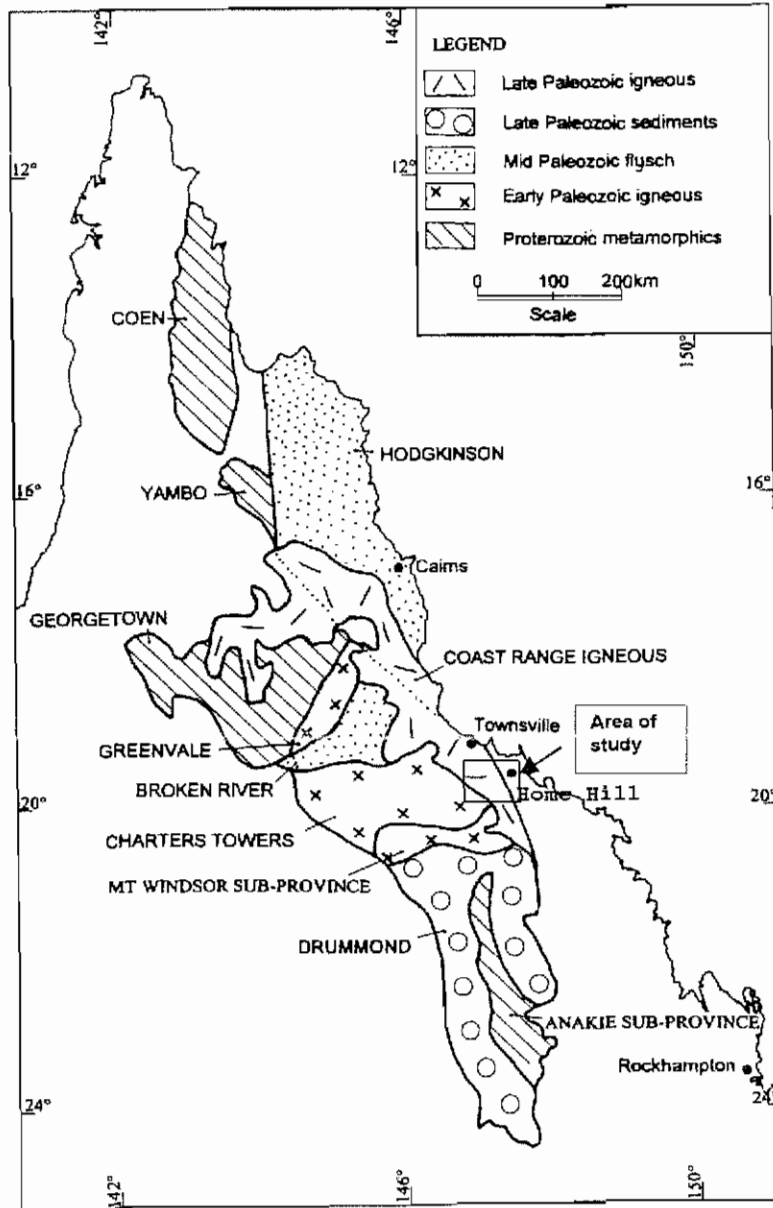


Figure 2.1. Geological Provinces and Subprovinces of Northeast Queensland, modified from the "Exploring the Tropics; Mineral Deposits of Northeast Queensland; Geology and Geochemistry" edited by S.D.Beams, 1995.

2.2. Correlations and Origin of Metamorphic Rocks

The largest package of the metamorphics known as the Cape River Metamorphics are Neoproterozoic or Early Cambrian in age according to the isotopic studies conducted by Withnall et al. (1997). The Cape River and Charters Towers Metamorphics consist of high-grade metamorphics and migmatite originated in the early to mid Ordovician. High-grade metamorphics in the Argentine Metamorphic are possibly formed at the same time (Rienks and Withnall, 1996; Draper, 1998).

A correlation between the Anakie Metamorphics and the Cape River Metamorphics is drawn by Withnall et al. (1995) and based on similar geochemical characteristics of amphibolites. The Cape River Metamorphics, Charters Towers Metamorphics and Argentine Metamorphics all include phyllite, schist and quartzite intruded by early to mid Ordovician S-type granites enclosed by medium to high-grade metamorphics. The same type of metamorphics could be found in the Cairns Region of the Barnard Metamorphics.

If these correlations are correct, late Neoproterozoic or Early Cambrian meta-sedimentary rocks form a belt from Cairns to central Queensland and possibly as far as southern Australia. Further correlation of these units by Withnall et al. (1995), suggested Delamerian age (Cambrian) for this sequence.

Because of the lack of evidence for depositional ages, two possible tectonic scenarios are suggested by Withnall et al. (1995).

- 1) The rocks in the Lolworth-Ravenswood block and Anakie Inlier possibly represent micro continents of Mesoproterozoic age that drifted off the Australian craton along the Diamantina Lineament and later amalgamated with the main craton.

- 2) Those units were deposited in the Neoproterozoic or Early Ordovician on the rifted continental margins of Gondwanaland during and after break up of Rodinia (Moore 1991, in Withnall et al 1995). This break-up took place either during the Early Cambrian (Dalziel 1991, in Withnall et al., 1995) or Neoproterozoic (Storey et al., 1992, in Withnall et al., 1995).

The metamorphic rocks of the Inkerman Shear Zone show similarities in structural orientation with the Argentine Metamorphics and possibly the Charters Towers Metamorphics. However, the tectonic significance of all of these metamorphic blocks must remain uncertain until more age dating becomes available.

Chapter Three

Local Geology

3.1. Introduction

The Inkerman Shear Zone represents a characteristic structurally anomalous series of lineaments with a west – southwest trend. Low outcropping ridges of calcsilicates, amphibolites and granitic gneiss represent these lineaments. Permo-Carboniferous dykes of various compositions form a dominant structural trend at right angles to the ridges. Broadly, the area mapped is represented by two suites of lithologies, which are interpreted to be of very different ages. The older unit is a metamorphic sequence and the younger is an igneous sequence.

3.2. Metamorphic Unit

This unit consists of various calcsilicate rocks, amphibolites and granitic gneiss. Amphibolite and calc-silicate rocks are generally east west trending and form a distinctive ridge system.

3.2.1. amphibolite

Throughout the study area, amphibolite outcrop is widespread and can be examined in the exposures in the old Trans Australian costeans. Amphibolite forms a banded rock consisting of alternating bands of dark green hornblende

and lighter coloured bands of plagioclase and quartz. These bands range in thickness from 2-3 mm to 6-7 cm. The alternating bands are not necessarily the same thickness and the rock can range from almost massive plagioclase-quartz with very thin hornblende bands to a rock with finely defined bands that are of uniform thickness. In the eastern part of the study area amphibolite forms larger bodies of almost massive plagioclase - quartz with very thin hornblende bands. Grain size ranges from fine to coarse. With increasing quartzo-feldspathic content, these rocks grade into strongly banded migmatite, which are exposed in the walls of the costeans.

The distinctive foliation of these rocks runs approximately east – west. In some places these rocks are intensely folded with fold axes having a fairly constant plunge and axial planes parallel to the foliation. The lineation that is present in the amphibolites pitches eastward at 35° within the foliation plane, which dips 85° towards 7°.

The amphibolites of this area display substantial variety in composition and texture. Generally, these rocks consist of 20-30% amphibole, 50% plagioclase, 2% quartz, 2% sphene, 5% opaque minerals and with evident chloritic alteration. Amphibole minerals come as elongated grains, which define a strong lineation within a foliation. The retrograde chlorite is parallel to the foliation.

In the amphibolite outcropping south west of the Inkerman homestead, Nisbet and Goulevitch (1970) observed structures, which suggested that the layering had been transposed. This led to the suggestion that the amphibolite is a regionally metamorphosed rock although Paine et al. (1964, in Evans 1991) suggested that these rocks represent a sheared version of a granodiorite found in the area.

3.2.2. calcsilicate rocks

Calcsilicates are widespread in the project area and usually form distinctive ridges striking parallel to the east – west foliation in the amphibolites. Generally, they are medium to coarse-grained, well-banded metasediments with distinct mineralogical layering (Figure 3.1.). Layering varies in thickness between 2 mm and 2 cm. Mineralogy also varies across layers and is dominated by garnet, clinopyroxene, epidote, hornblende, plagioclase, quartz and calcite. These rocks also contain varying amounts of wollastonite, feldspar, diopside and titanite. In outcrop the carbonate rich layers are often more deeply weathered leaving the more resistant silica layers to stand out.



Figure 3.1. *Banded calcsilicate showing distinctive quartz-feldspar rich layers (white-orange) and diopside rich layers (green). Pencil provides the scale. (Taken from Foster, 1994).*

The calcsilicates contain widespread pegmatitic veining that in some instances cross cuts the general layering of calcsilicate rocks (Figure 3.2.).

The calcsilicate layers dip steeply 70-85° to the north-northwest and show evidence of multiple deformations with small parasitic folds striking east-west. The layering is parallel to the foliation of the other lithological units. In some instances garnet layers are boudinaged, forming pods slightly rectangular in shape and 2 to 3 cm thick. Some of these pods show evidence of strong sub horizontal east-west shearing.



Figure 3.2. *Banded calcsilicate outcrop with pegmatitic veins crosscutting the layering. Note some pegmatitic veins that run parallel to the layering.*

The calcsilicate rocks crop out in a variety of ways. This unit in some locations forms pod like areas where the sedimentary layering cannot be distinguished (may not be present) as can be seen in the Figure 3.3.



Figure 3.3. *Calcsilicate outcrop with a very fine layering (possibly foliation). The outcrop is dominated by wollastonite and garnets.*

These areas are dominated by garnet and wollastonite and usually form small outcrops about one metre in diameter but occasionally can form larger outcrops.

3.2.3. granitoid gneiss

Rocks belonging to this unit were originally of granite to granodiorite composition. Patches of the original igneous texture could be recognised in thin sections. This lithological unit shows strong gneissic layering and displays east – west foliation similar to the foliation developed in the amphibolite and calcsilicate unit. The layers differ in thickness from 2 mm to 2 cm and consist of quartz, plagioclase and K-feldspar layers alternating with diopside rich layers

and varying amounts of garnet. Some of these layers contain isoclinal folds. It has been interpreted that these layers are granitoid veins, which have intruded calcisilicate rocks. In general, rocks that form this unit are medium to coarse grained with quartz and plagioclase grains up to 2 mm and diopside grains generally much smaller at 0.25 mm. Some layers are completely deficient in garnet minerals and in some layers garnets develop pod like forms. Other minor minerals incorporated in this lithological unit are hornblende, potassium feldspar, epidote, sphene, magnetite and pyrite.



Figure 3.4. Granitic gneiss showing foliation and numerous xenoliths of a metasediment, foliation is S_2 .

3.3. The Intrusive Rock Unit

The younger sequence is presented by a group of late granitoids, syenogranites and mafic dyke unit.

3.3.1. granitoid veins

These rocks occur as abundant veins and small pods throughout the calcsilicate and are usually medium to coarse grained. Their general strike is between 75 to 80° , with the dip towards north at approximately 80° . They are weathered and commonly very leucocratic. These rocks are composed of 40% quartz, 35% plagioclase, 20% potassium feldspar and minor hornblende, biotite, magnetite and sphene. Hornblende crystals vary in size from 0.5 to 6 mm. If alteration is evident, it is usually sericite and chlorite alteration. The rocks of this unit show a near vertical foliation that trends east – west with varying intensity. This foliation is defined by the alignment of the hornblende and biotite grains. The foliation can be seen in a thin section of the leucocratic granite (Ink6) where quartz has been recrystallised to a finer grained matrix, which include amoeboid grains that define foliation (Figure 5.14. chapter five).

3.3.2. leucocratic syenogranite

This rock unit forms a separate body and is represented by medium to coarse-grained intrusive rock that outcrops in the far southeasterly part of the area. The colour is usually light pink but also come in shades of light grey. It shows typical coarse-grained igneous texture with an average grain size of 1–3 mm. These rocks are composed of homogranular potassium feldspar (40%), plagioclase (10%) and quartz (45%). Present is also a small content of biotite, minor garnet and opaques (1%). Signs of minor alteration occur in the form of

small vugs that are filled with calcite. Where present, muscovite was formed by the breakdown of biotite and surrounds larger grains of quartz and feldspar. It appears that the garnets have been formed by the breakdown of a ferromagnesian mineral. Outcrops of this unit that are closer to the metamorphic unit appear to be slightly foliated. Further south, foliation is less evident (Figure 3.5.). For these rocks an upper Permian age was proposed by Paine et al. (1970) but this is unlikely given its foliation. Foliation in this rocks is steep, so is either S_4 or S_2 . Therefore, these rocks could be formed during or before the last ductile deformation event. Real Permian granitoids in the region are unfoliated.

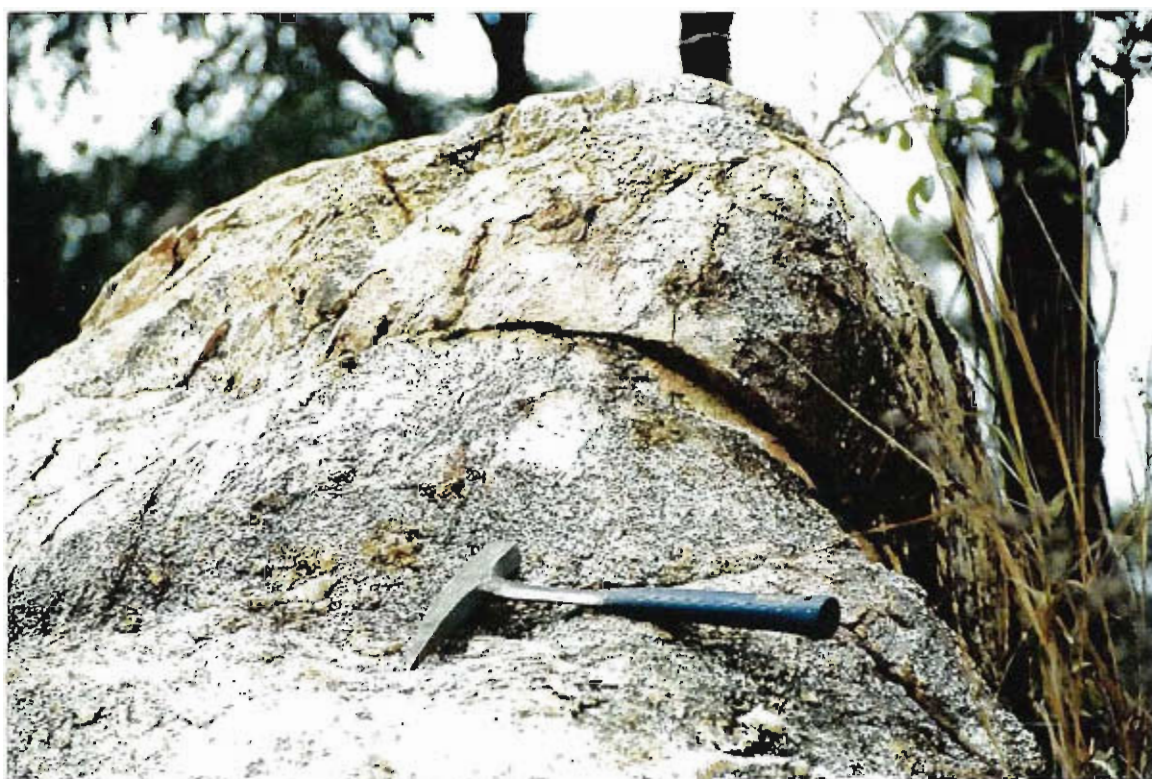


Figure 3.5. *Outcrop of a pink syenogranite rock, lightly foliated. A hammer provides the scale.*

3.3.3. mafic dykes

Abundant dykes, with compositions from andesite to diorite to basaltic, make up this rock unit. These dykes have intruded all other lithologies of the area. They have a constant strike, which ranges between 320° to 340° and dip east at approximately 80° (Figure 3.6). The dykes range in width from a few centimetres to a few metres but are usually 20 cm to 1 m wide. Most are fine to medium grained although coarse-grained porphyritic dykes can be found in the southern part of the project area (Foster, 1994).



Figure 3.6. A mafic dyke crosscutting calcsilicate rock, strikes 320° and dips 80° towards east. A hammer provides the scale (the photo taken from Foster, 1994).

The dykes are dominated by hornblende and plagioclase with the grain size averaging 1 mm. The hornblende content varies from 30 to 60%, plagioclase ranges between 30 to 45% with significant quartz content. Plagioclase grains

are short prisms and show zoning with the core being richer in anorthite content. Accessory minerals are sphene, apatite and magnetite.

Feldspars from these dykes show chlorite and epidote alteration and in some instances are partly altered to sericite. If calcite is present it appears to be a late replacement of former chlorite filled voids.

The dyke rocks of this unit have no evidence of foliation or any other deformation and obviously postdate the formation of the foliation that can be found in the host lithological units such as amphibolites, calcsilicates and gneiss. According to Stephenson (1990) these dykes are part of the Permo-Carboniferous mafic dyke swarm that is found along the east coast of Australia.

Chapter Four

Structural Geology

4.1. Introduction

Strongly foliated and deformed rocks are widely spread in the study area and show distinctive character of a high-grade regional metamorphic origin. Faulting of the Inkerman Metamorphics is evident on the micro and macro scale. Macro scale faulting is visible on the aerial photographs showing the displacement of the major lineaments and topographical units. Evans (1991) stated that some breccia zones were found during the field mapping. None of these rocks were found in the study area.

In the study of the northeastern part of the Lolworth-Ravenswood sub-province, Withnall and McLennon (1991, in Withnall et al., 1995) identified two major deformation events that could be compared with S_1 and S_2 foliation that are found in the rocks of the Inkerman Metamorphics.

4.2. Second Deformation Event (D_2)

The common foliation fabric that can be noted in calcsilicates, amphibolites and granitic gneiss has been termed S_2 and is generally oriented east - west. In Figure 4.1., which represents layered calcsilicates with alternating quartz-felspathic layers and garnet layers, S_2 can be noted. At the same time some of the original foliation S_1 can be observed. S_2 foliation is observed in the granitic

gneiss, which crop out in the southern part of the study area and can be seen in Figure 3.4. (Chapter three).



Figure 4.1. *Banded calcsilicate rock showing S_2 foliation with some evidence of S_1 foliation preserved in original layering. Visible are garnet boudins to the left and to the right of the lens cover.*

Most of the rocks observed in the study area showed the evidence of multiple folding events. Small parasitic folds, striking east-west, are evident in calcsilicate outcrops. These folds can be interpreted as F_2 and some of possible F_3 generation. Evidence for F_2 folds can be seen mostly in south-westerly part of the study area. Figure 4.2. shows F_2 and a late granitic vein in calc-silicate outcrop. Figure 4.3. illustrates F_2 folds with foliation S_1 that is parallel to S_0 visible in the hinge.

A prominent lineation found in the study area is represented by the elongated direction of hornblende grains on a foliation surface in amphibolite. It pitches eastward at 35° within the S_2 foliation $85^\circ \rightarrow 007^\circ$. The same foliation can be noted in the deformed granite, which outcrops on the southern side of the ridge and is represented by elongated biotite crystals.



Figure 4.2. A calcsilicate rock with a pegmatitic vein folded by the F_2 fold. The pegmatite intruded post D_1 and pre or early syn- D_2 .

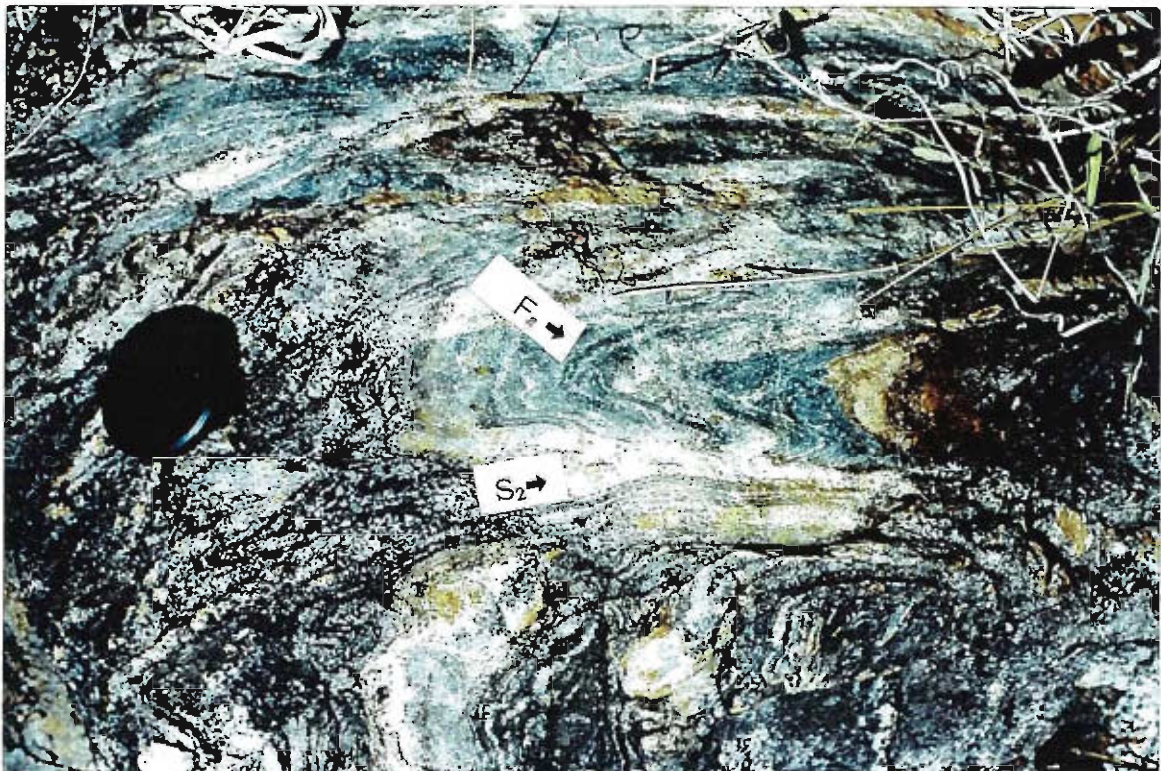


Figure 4.3. F_2 fold in calcsilicate with visible foliation S_1 and S_0 in the hinge. Granite layers with S_2 .

4.3. Third Deformation Event (D3)

During this deformation event an S_3 axial plane foliation was locally observed. This is evident in calc-silicate outcrops and shows an east-west trend. In the same event rocks are folded and F_3 folds can be noted in Figure 4.4. with S_3 axial planes that are gently dipping.

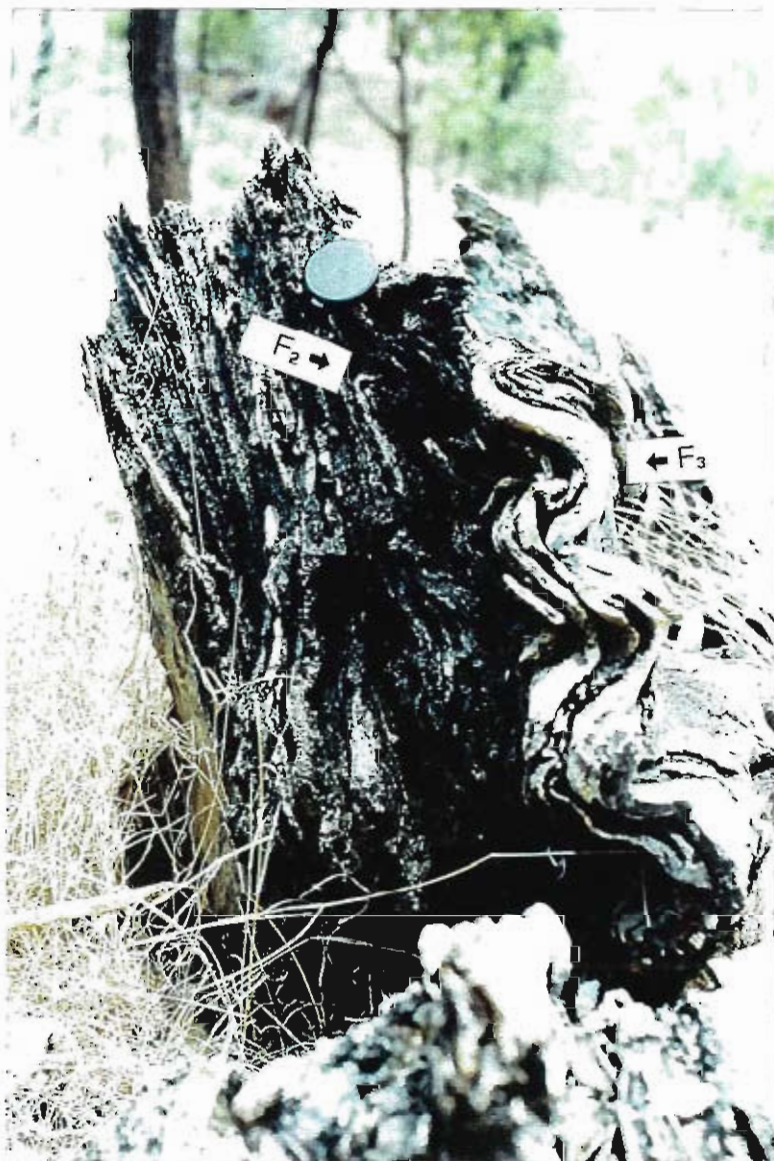


Figure 4.4. F_2 and F_3 folds developed in calcsilicate and showing shallowly dipping S_3 axial planes in flat folds.

In Figure 4.5., a calcsilicate outcrop with multiple folding events, with smaller parasitic folds of possible F_3 generation (shallow) and folds of possible F_4 generation (steep).

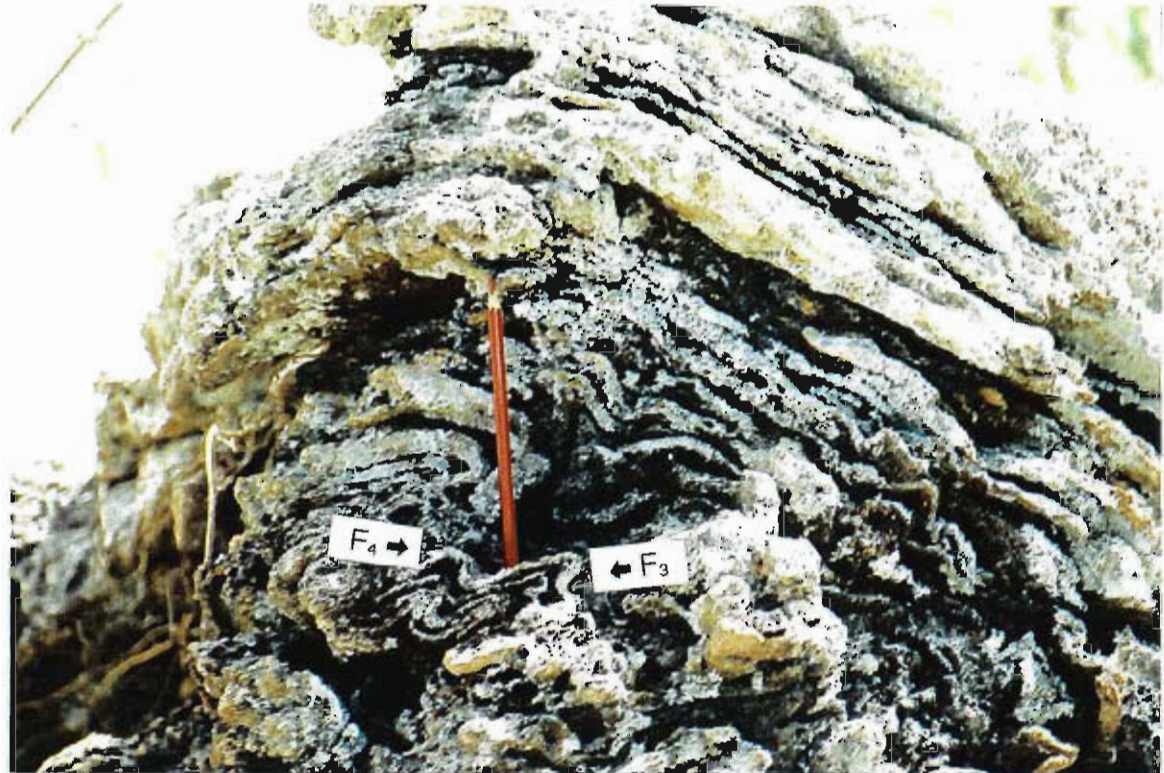


Figure 4.5. A photo showing folded calcsilicate rock with more resistant silica rich layers and deeply weathered carbonate layers with three fold generation. The F_3 folds exhibit shallowly dipping axial planes whereas the axial planes of F_4 folds are steep.

F_3 anticline plunge is 52° towards north-northwest. Parasitic folds indicate that a larger anticline structure is to the north.

The flat folds that have a plunge of 21° towards north-northwest are F_3 . The associated S_3 axial plane is $23^\circ \rightarrow 291^\circ$.

4.4. Fourth Deformation Event (D4)

This was observed as folds with steep axial planes superimposed on F_3 folds (Figure 4.5.). It is noted that in leucocratic syenogranite the foliation is less intense than in the rocks of the metamorphic unit. In these rocks the foliation is defined by the alignment of the hornblende and biotite grains. In syenogranite elongated quartz grains define foliation and this foliation is interpreted as S_4 .

4.5. Other Structural Characteristics

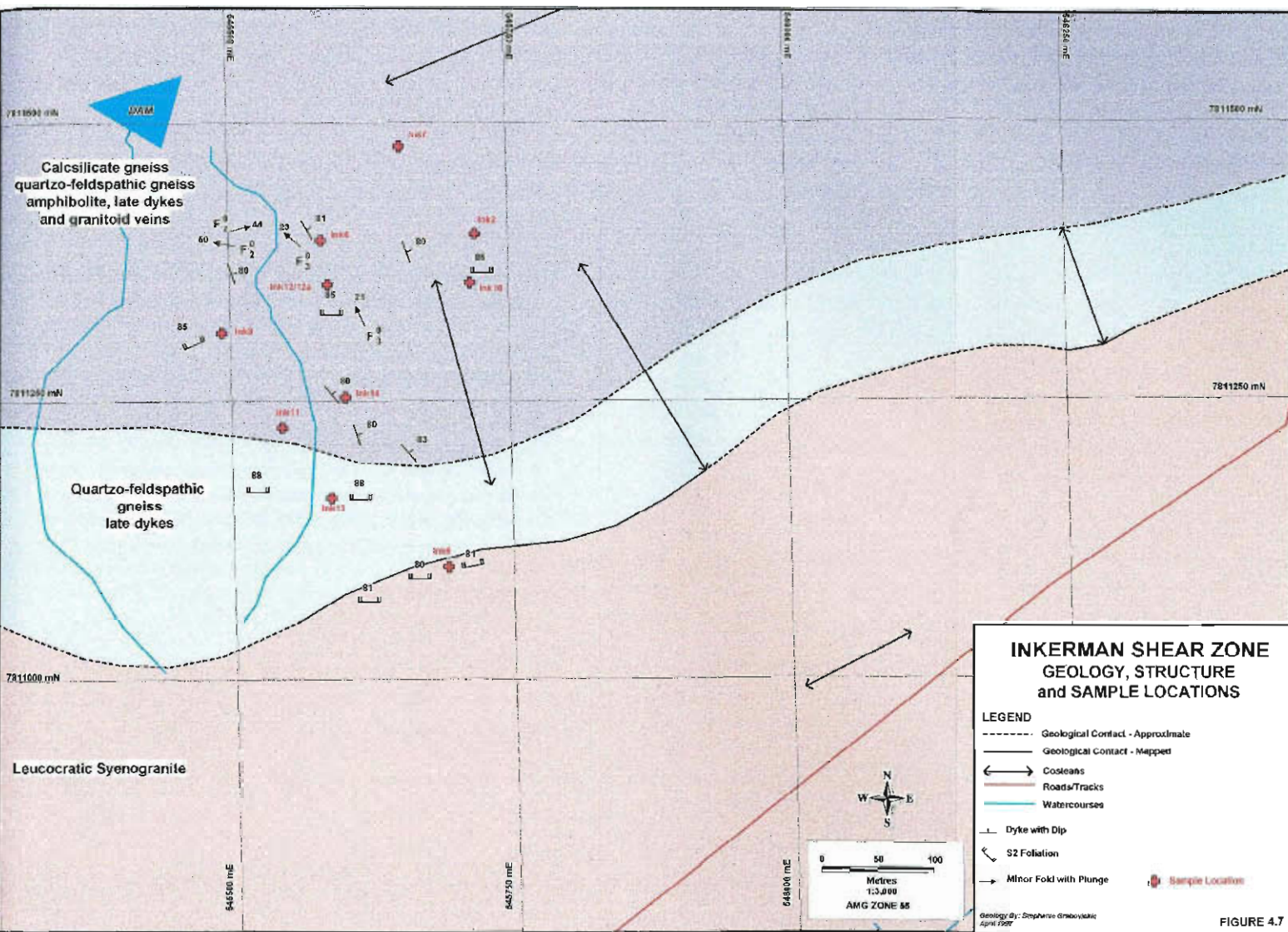
It is previously noted that boudinaged garnet and calcite pods can be seen in the calc-silicate unit. Generally these pods are slightly lenticular in shape and they occur in such a way that the layering is deflected around the pods. Some of these boudins appear to show east-west sub horizontal direction of shearing. This can be seen in Figure 4.6. where a sheared garnet pod shows some brittle fractures crosscutting the pod.

In the late crosscutting pegmatitic veins can be found mylonitic texture with new grain development anastomosing around larger crystals. This texture can be seen in Figure 5.5. (chapter five) of a pegmatitic vein in the gneissic rock.



Figure 4.6. *Oriented banded calcsilicate specimen with a garnet pod showing strong foliation in a sub horizontal orientation and crosscutting fractures. (Taken from Foster, 1994).*

Mafic dykes that have intruded all other lithologies dip east at 80° and strike north-northwest show no evidence of foliation. The correlations of these dykes (Stephenson, 1990) with the Permo-Carboniferous mafic dyke swarm suggest a regional fracture-opening regime during a major extensional period. This event postdates the development of the east-west foliation found in D_3 .



INKERMAN SHEAR ZONE GEOLOGY, STRUCTURE and SAMPLE LOCATIONS

LEGEND

- Geological Contact - Approximate
- Geological Contact - Mapped
- ↔ Costeans
- Roads/Tracks
- Watercourses
- Dyke with Dip
- ↙ S2 Foliation
- ↘ Minor Fold with Plunge
- Sample Location

N
 W —+— E
 S

0 50 100
 Metres
 T33,898
 AMG ZONE 55

Geology By: Stephen Griboskiak
April 1997

FIGURE 4.7

Chapter Five

Petrology and Mineral Chemistry

5.1. Introduction

The origin of calcsilicate rocks, skarns and other metamorphic rocks are considered by such authors as Jamtveit, Barton, Einaudi, Kwak, Newberry, Powell, Holland, Yardley and many others (see Reference List).

Metamorphosed and metasomatised lithologies that are exposed in the area mapped are interpreted as originally carbonate rich sediments and felsic igneous intrusions. Some of the rocks in the area have undergone skarn development. A detailed laboratory examination of the thin sections defined the mineral assemblages and micro-structural characteristics of the lithological units. Selected polished sections were submitted to the electron microprobe at the JCU microprobe laboratory (Jeol microprobe, EDS analysis). The analytical results are presented in Tables 2 – 8 (Appendix 1). The results were averaged if there was no significant zoning within crystals or differences between individual crystals. For the garnets and the pyroxenes Fe was allocated to Fe²⁺ or Fe³⁺ using a stoichiometric program. The thin sections are described and presented in Appendix 2.

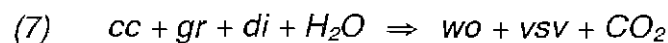
5.2. Calcsilicate Assemblages

A number of calcsilicate mineral assemblages were observed from this area and are presented in Table 1.

Table 1	Calcsilicate mineral assemblages
1.	Wollastonite, garnet, vesuvianite, calcite, diopside (rim of garnet in Ink2 only)
2.	Wollastonite, garnet, calcite, diopside
3.	Wollastonite, garnet, diopside, calcite, scapolite, tremolite*
4.	Quartz, plagioclase, pyroxene, garnet, epidote*
5.	Quartz, plagioclase, diopside, hornblende
6.	Quartz, plagioclase, epidote*, hornblende, magnetite
7.	Quartz, plagioclase, K-feldspar, prehnite*
8.	Quartz, plagioclase, diopside, garnet, hornblende
9.	Garnet, plagioclase, pyroxene, quartz
* retrograde minerals	

5.2.1 calcsilicate rock with wollastonite, garnet, vesuvianite, diopside and calcite

The groundmass of this rock (Ink2) consists mainly of wollastonite with minor of diopside, calcite and titanite. It also contains subhedral garnet porphyroblasts up to 6 mm diameter. Microprobe analysis of garnets from the selected polished sections indicated that all garnets are grossularite – andradite. Although garnet crystals showed zoning in relation to the size of inclusions there is no zoning in chemical composition. Ink2 shows garnet composition varying from Gr₇₆An₂₁ to Gr₈₀An₁₅ but with no obvious difference from core to rim. Garnets in these rocks contain various inclusions of the ground mass minerals wollastonite, vesuvianite, diopside, and titanite, (Figure 5.1 and Figure 5.2). The outer rims consist of abundant wollastonite grains with vesuvianite grains placed on the core-rim boundary. Wollastonite was not found in the garnet core, where the inclusions are all diopside. Reaction (7), which produced vesuvianite and wollastonite, appears to have occurred at the core-rim boundary. On the larger scale the wollastonite matrix shows a strong S₂ foliation whereas inclusions in garnet are random. It seems that S₂ formed after garnet growth. Note also the dramatic grain coarsening from core to rim to matrix (Figures 5.1 and 5.2).



Clinopyroxene inclusions found in this specimen were microprobed in relation to garnet core-rim position and showed no zoning in chemical content. All clinopyroxene probed were Mg rich diopside (Di₈₈Hed₁₂).

Figure 5.1. Photomicrograph of Ink2 showing a garnet porphyroblast in wollastonite groundmass. Note that garnets show distinct core-rim, where inclusions show zoning in grain size. The outer rims contain abundant acicular wollastonite grains where as in the garnet core wollastonite is not found. Vesuvianite grains are mainly at the rim-core boundary. Note the dramatic change in grain size of inclusions at the core-rim boundary (X-polarized light, length 5.6 mm)

Figure 5.2. Photomicrograph of Ink2 showing garnet porphyroblast in wollastonite groundmass. Note the dramatic change in grain size of inclusions at the core rim boundary showing large vesuvianite grains (X-polarized light, length 2.8 mm)



Figure 5.1. *Photomicrograph of Ink2*

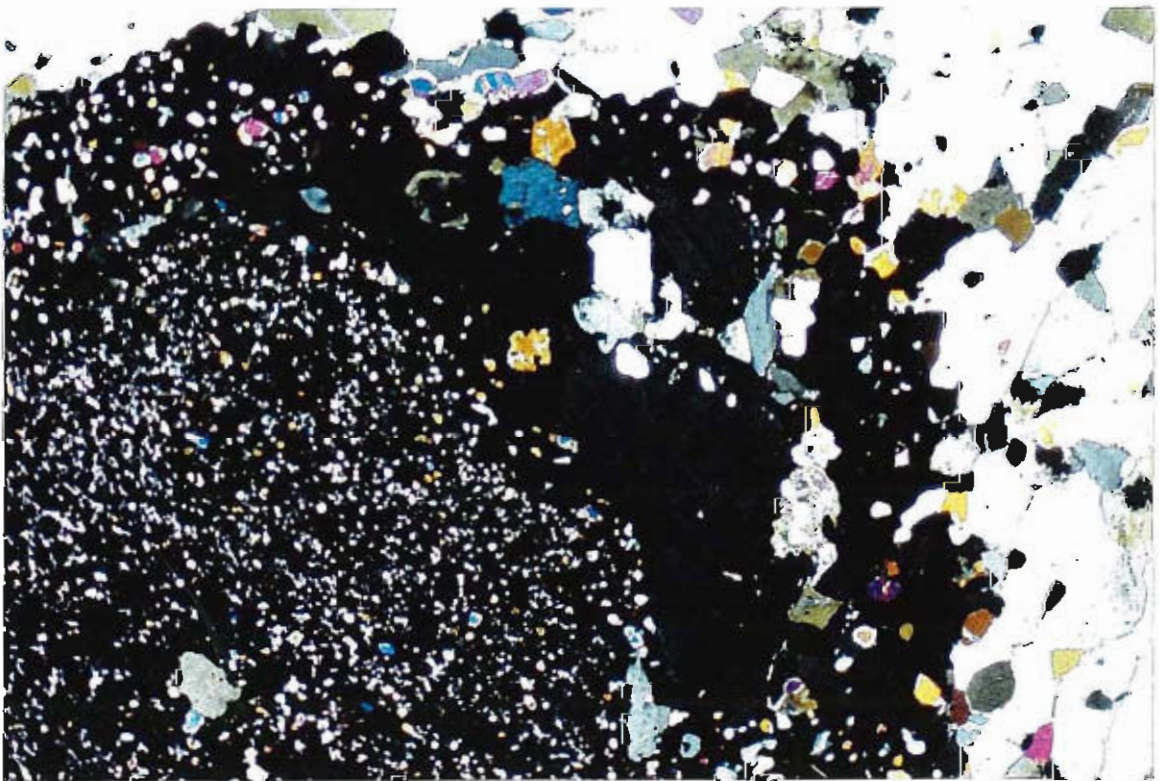


Figure 5.2. *Photomicrograph of Ink2*

5.2.2. calcsilicate rock with quartz, plagioclase, pyroxene and epidote

Layered calcsilicate rock of this composition is one of the most common calcsilicate rocks. This rock consists of alternating granite-tonalite layers and mafic layers. The main minerals in tonalite layers are coarse-grained quartz, plagioclase with minor clinopyroxene, epidote and titanite. Mafic layers consist mainly of plagioclase, clinopyroxene, quartz and titanite (Figures 5.3 and 5.4.). The clinopyroxene is believed to have an endoskarn origin, along with the plagioclase of labradorite/bytownite composition.

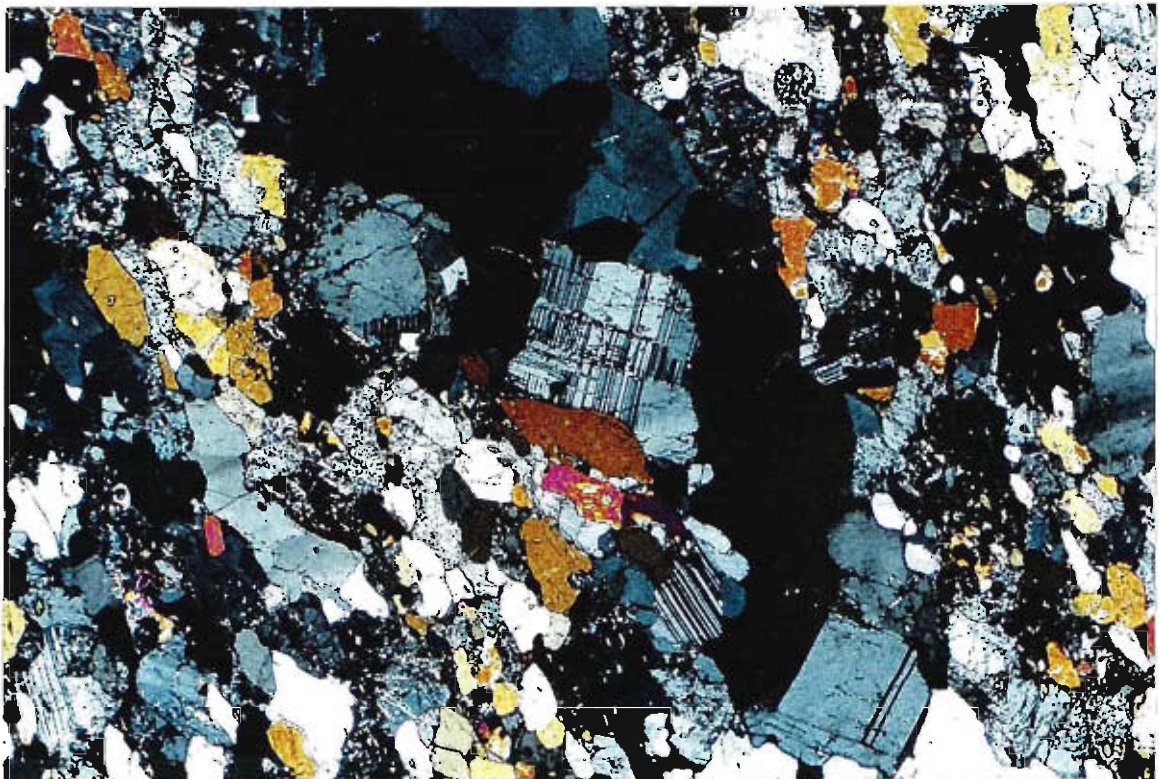


Figure 5.3. Photomicrograph of Ink11 showing a typical layered calcsilicate rock with coarse-grained pegmatitic vein and alternating mafic layers consisting of clinopyroxene, plagioclase and quartz. Note the strong S_2 foliation subparallel to the layering (X-polarized light, length 2.8 mm).

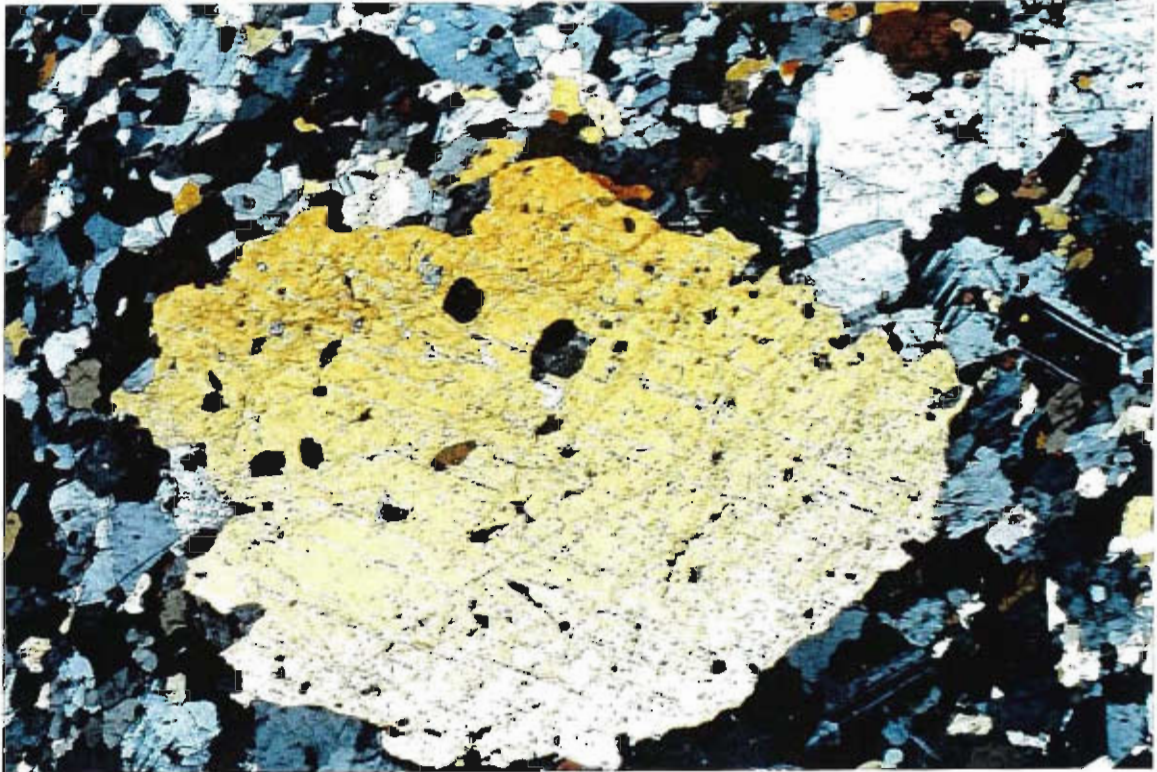


Figure 5.4. Photomicrograph of Ink12 showing a very large pyroxene grain within a granitic layer. Note titanite inclusions within the pyroxene grain (X-polarised light, length 2.8 mm)

Thin section HH7 of a pegmatitic vein in a calcsilicate rock (taken from Foster, 1994) shows a well-developed mylonitic texture where quartz has been recrystallised (Figure 5.5.).

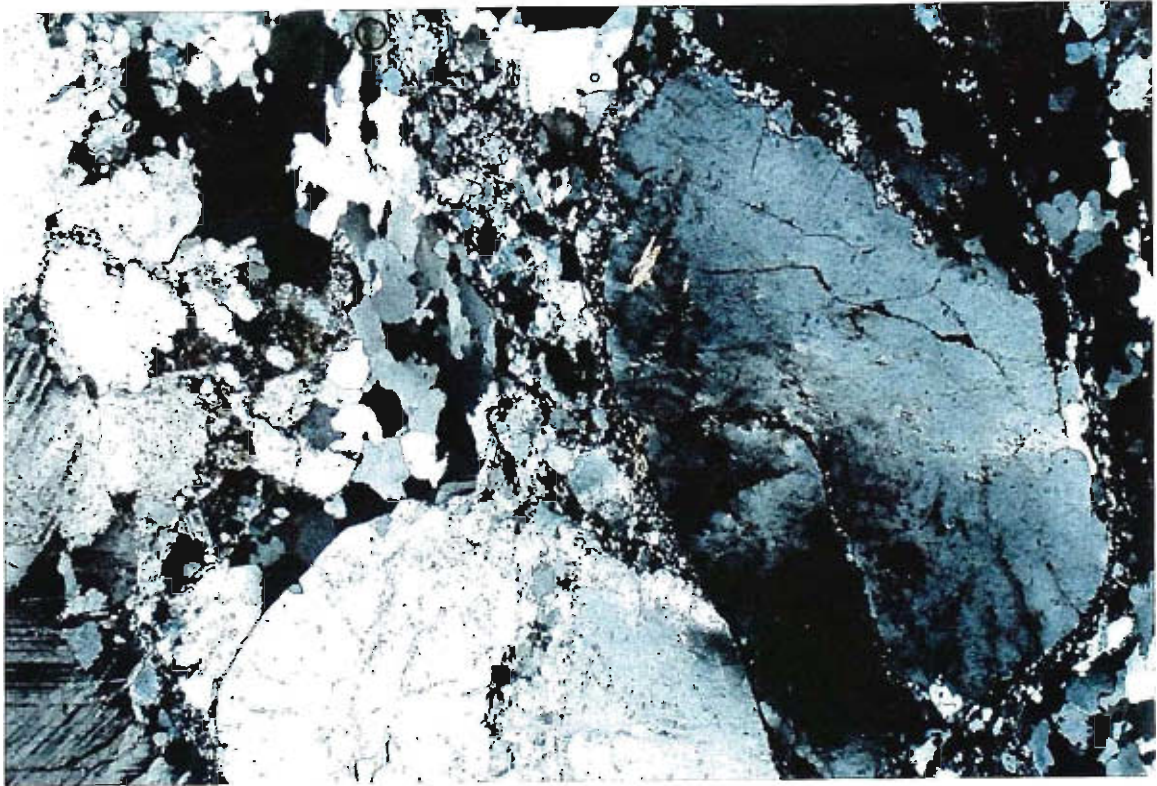


Figure 5.5. Photomicrograph of HH7 with mylonitic fabric development represented by a new grain development and pressure shadows around large quartz grains in a pegmatitic vein. As quartz grains have not been totally recrystallised it is suggested that the intrusion was late or post D_2 (X-polarised light, length 2.8 mm).

Some layered calcsilicates have alternating diopside and quartz/plagioclase layers where elongated diopside and plagioclase grains define strong S_2 foliation as can be seen in Figure 5.6. The clinopyroxene appear to be variable in composition as in some layers shows deep green and light green in others.

Allanite was found in one of the pegmatitic veins found in layered calcsilicates (Figure 5.7.) This specimen was analysed by Foster (1994) and was found to contain significant amounts of cerium and thorium (analysis Ba9).

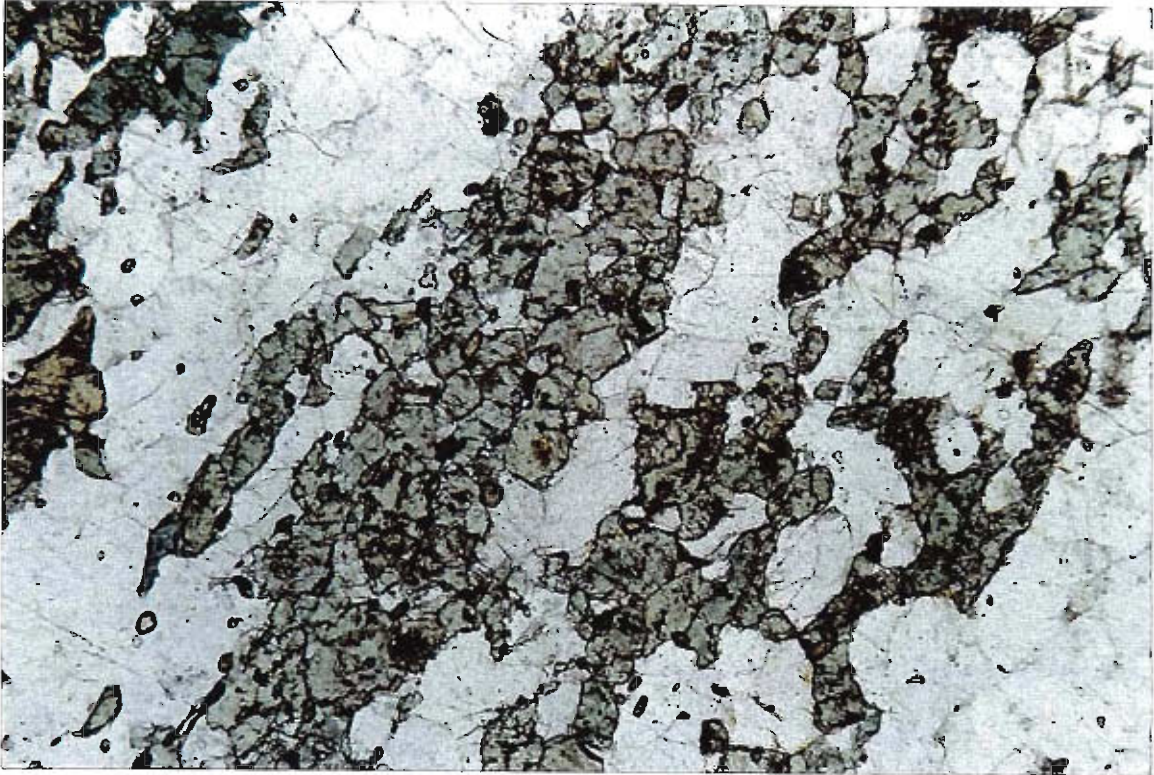


Figure 5.6. photomicrograph of HH4 with a strong foliation defined by elongated clinopyroxene grains. Note numerous titanite inclusions (p. polarised light, length of photo 2.8 mm).

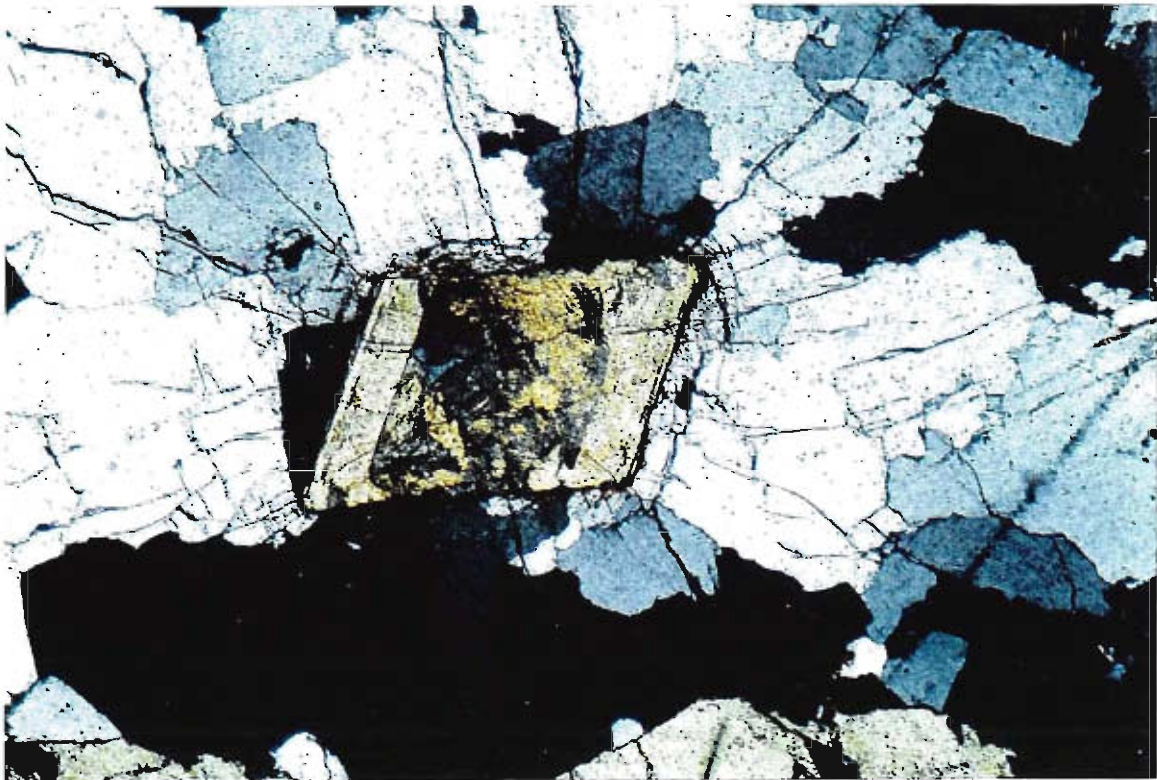


Figure 5.7. Photomicrograph of HHA9 showing an allanite grain in pegmatitic vein. Note distinctive zoning and radiating expansion cracks formed on cooling (X-polarized light, length 2.8 mm).

Epidote comes in a form of thin epidote veins or fills in spaces between garnet crystals. It appears that epidote replaced garnet along irregular fractures and atoll structures as can be seen in Ink12 and Ink12a (Figure 5.8.). It is therefore interpreted as a retrograde mineral.

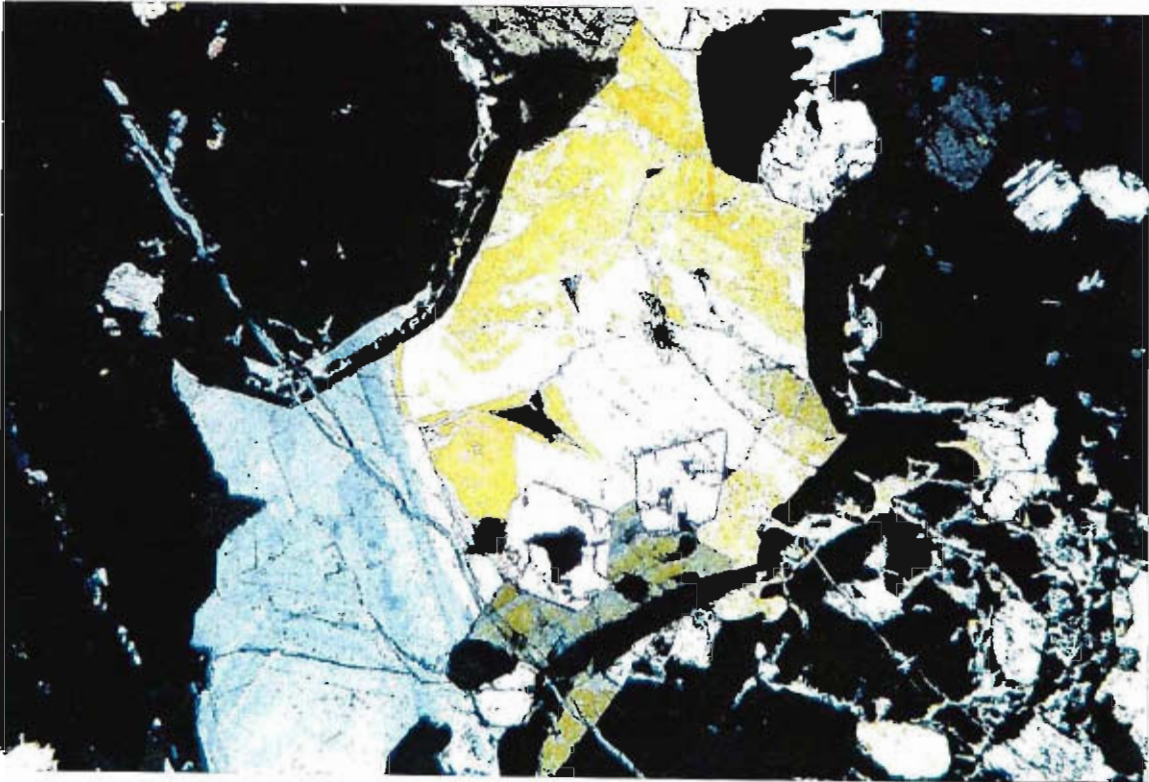


Figure 5.8. Photomicrograph of Ink12 showing clinozoisite infill between the atoll structures in garnets. Note orange and anomalous blue birefringence colours of this epidote family mineral (X-polarised light, length 2.8 mm).

5.2.3. other calcsilicates

Most calcsilicates observed were fine to medium grained layered calcsilicates, where layers vary in size from 0.1 to 0.5 cm. In some instances massive garnet layers are up to 1 cm thick. All garnets probed are grossularite – andradite with a low spessartine component and range from $Gr_{66}An_{32}$ (Ink10) to $Gr_{80}An_{19}$ (Ink13). One probe of garnet from Ink13 came with $Gr_{57}An_{40}Sp_3$. Garnets from these layers together with wollastonite defined a strong S_2 foliation.

Quartz, plagioclase and clinopyroxene layers usually form granitic layers and also define a strong S_2 foliation. These layers vary in thickness from 0.8 to 1 cm. All clinopyroxenes probed were diopside and ranged from $Di_{73}Hed_{27}$ (Ink8) to $Di_{84}Hed_{16}$ (Ink13).

The majority of plagioclase within the layered calcsilicates was anorthite end member varying from $An_{51}Ab_{48}$ (Ink8) to $An_{90}Ab_9$ (Ink13). One analysis of Ink13 showed very low anorthite content of $An_{43}Ab_{56}$. In some instances plagioclase is altered to epidote-clinozoisite (Ink11) or to sericite and saussurite (Ink8, HH1, HH2). In one of the pegmatitic veins (HHA7) alteration of feldspars to prehnite was evident (Figure 5.10). An unusual scapolite was probed (Foster 1994) and had a meionite composition of Me_{78} . These scapolites had a very high sulphur content estimated at around 3% (Figure 5.9.).

Epidote is a common late stage mineral found in calcsilicates of the study area. Epidote and clinozoisite occur commonly in veins crosscutting prograde skarns. Microprobe results from Ink15 showed that there was no zoning in epidote composition.

Titanite and magnetite come as accessory minerals. Pyrite and pyrrhotite were found as small inclusions in Ink8 and Ink12.



Figure 5.9. Photomicrograph of H3 showing a large scapolite grain wrapped by garnet and quartz. Garnet contain abundant inclusions of diopside and less significant quartz and calcite (X-polarised light, length 2.8 mm).

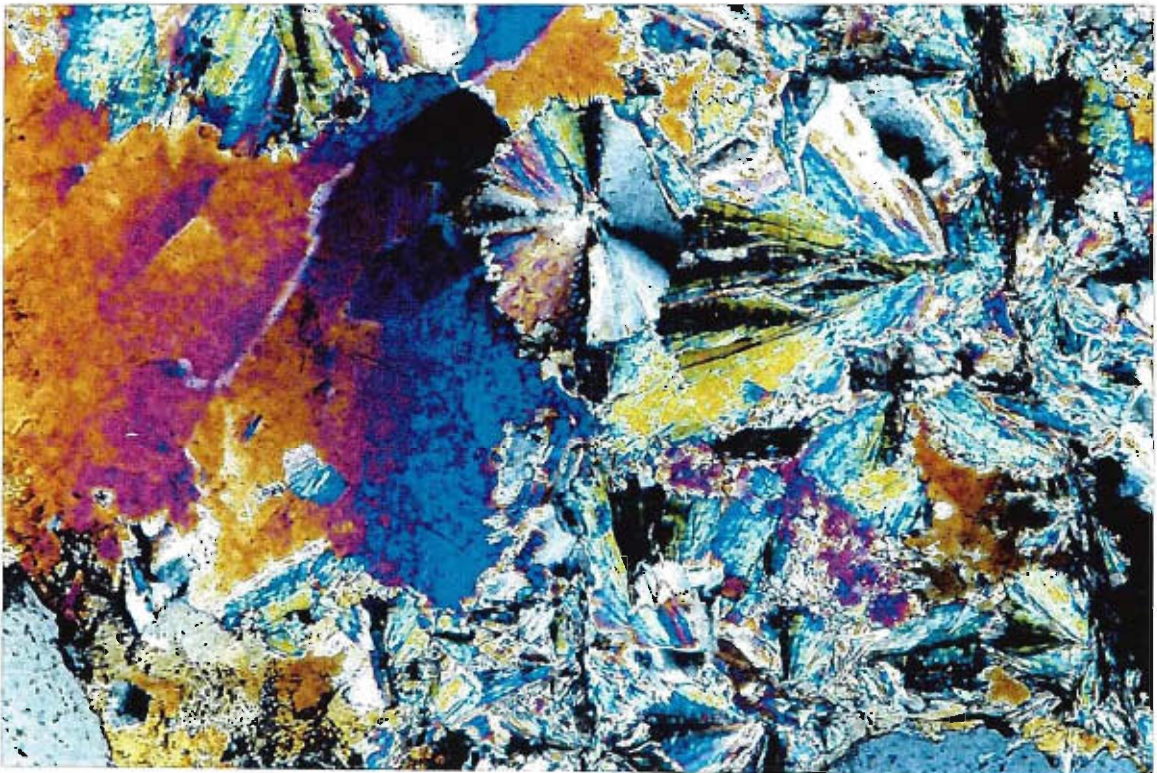


Figure 5.10. Photomicrograph of HHA7 showing a pegmatitic vein in a calcsilicate. The whole field of view is filled by one crystal of possible feldspar, now almost completely converted to prehnite (X-polarised light, length 5.6 mm).

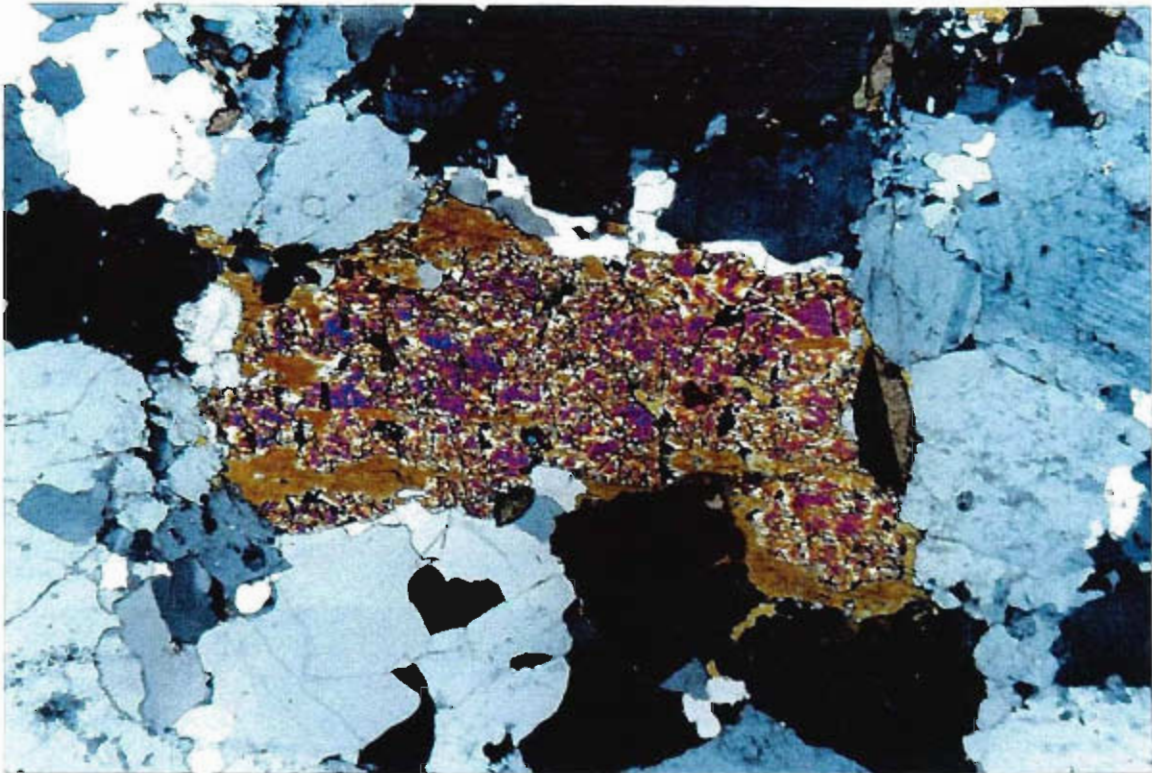


Figure 5.11. Photomicrograph of HHA12 showing an endoskarn development in monzogranite. Large hornblende grains are mostly broken down to pyroxene, titanite and opaque mineral (X-polarised light, length 2.8 mm).

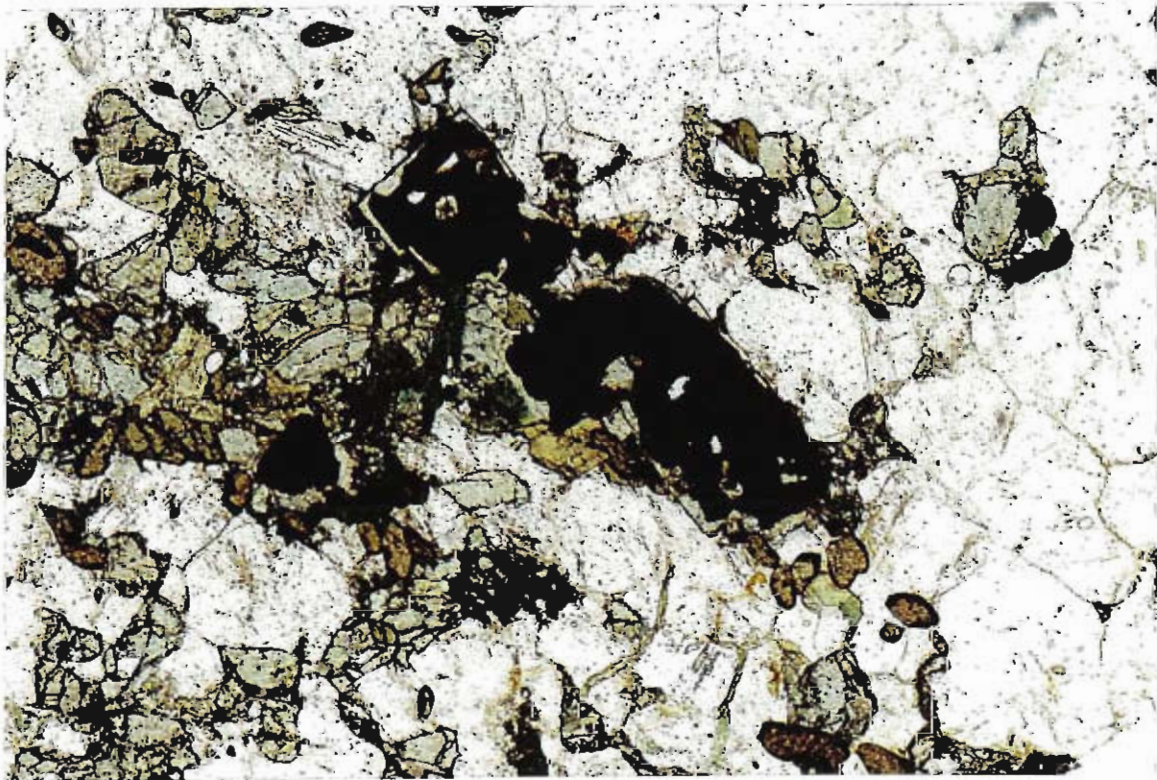


Figure 5.12. Photomicrograph of Ink8 showing layered calcsilicate where epidote and titanite are replacing magnetite. Amphibole and pyroxene define S_2 foliation (X-polarised light, length 5.6 mm).

5.3. Amphibolite

This mineral assemblage is represented by medium to coarse-grained altered plagioclase, amphibole, chlorite and minor quartz, titanite and opaque minerals. Amphiboles vary in colour from green to brown in plane polarised light. Elongated amphibole grains define strong S_2 foliation. The retrograde chlorite is also parallel to the foliation. Some pyrite inclusions were found and titanite occurs as very fine-grained patches.

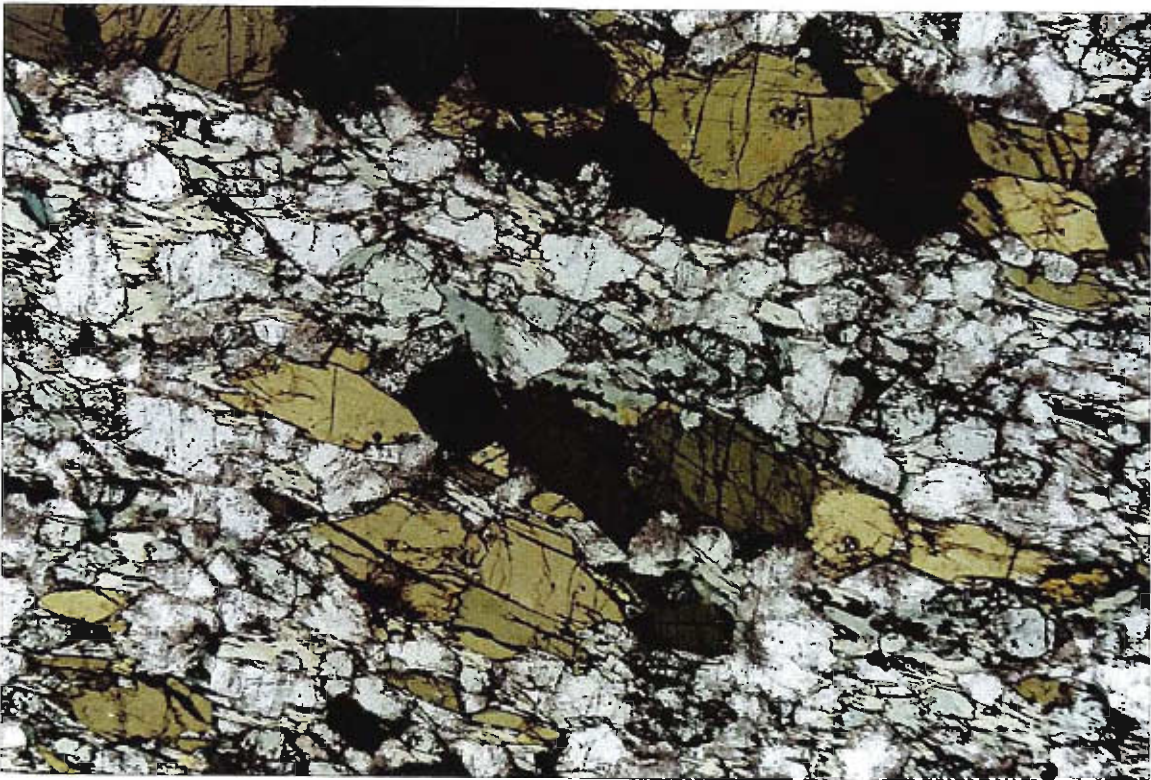


Figure 5.13. Photomicrograph of Ink7 showing elongated amphibole grains in green and brown colour that define the S_2 foliation (plane polarised light, length 2.8 mm).

Microprobe analysis of plagioclase from this specimen showed that plagioclase is albite 52%, anorthite 46 % and K-feldspar 1%.

5.4. Leucocratic syenogranite

This mineral assemblage is represented by quartz, K-feldspar, plagioclase and minor biotite, titanite, hornblende and magnetite. In thin section K-feldspar showed microcline and perthite. Generally, it is a fresh rock with little sericite alteration. In some instances biotite fills in the spaces between feldspars. Quartz has been recrystallised to finer grained matrix, which include amoeboid grains that define weak foliation (Figure 5.14).

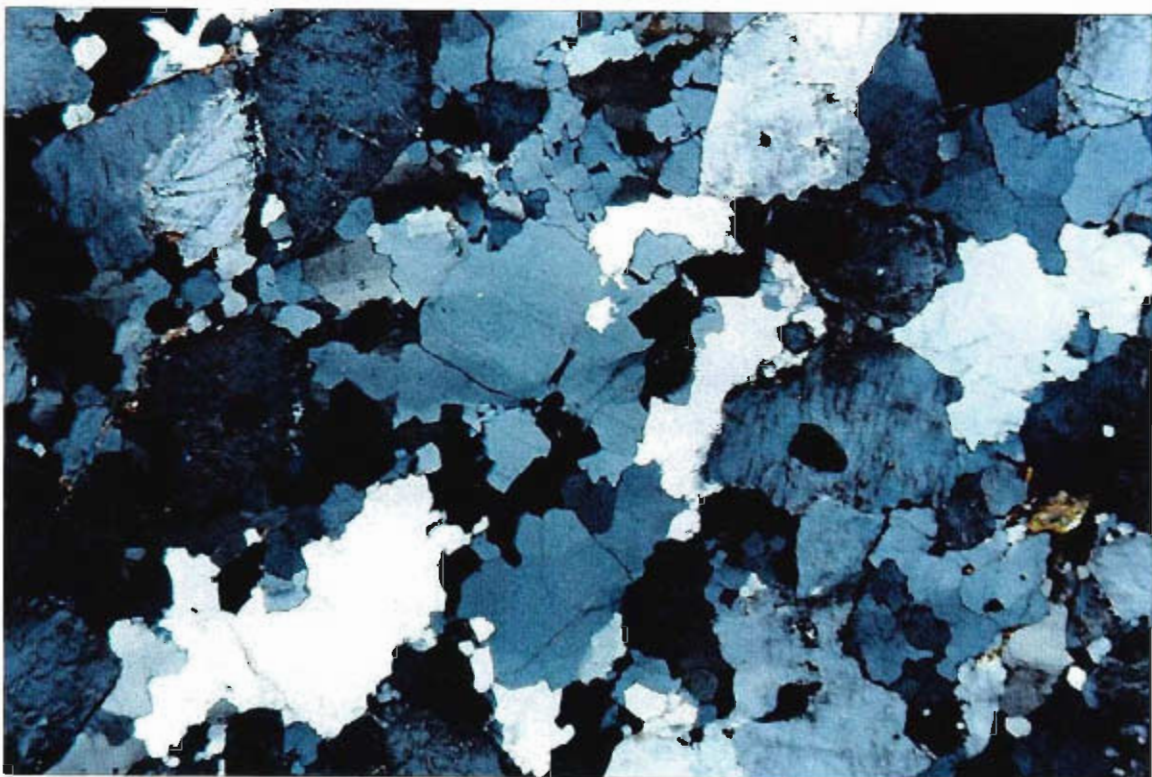
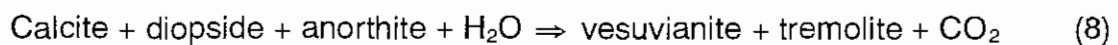
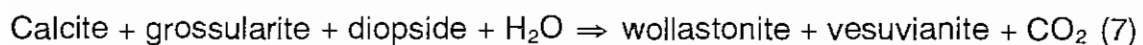
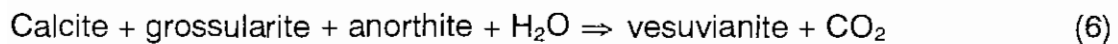
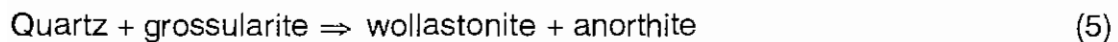
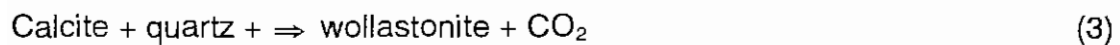
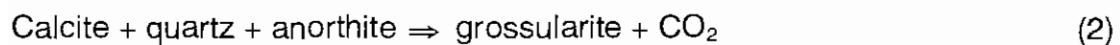
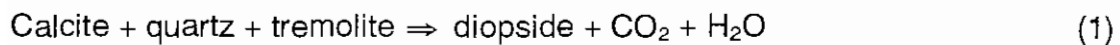


Figure 5.14. Photomicrograph of Ink6 showing a typical medium grained igneous texture of the leuco granite. Quartz grains show weak foliation (plane polarised light, length 2.8 mm).

5.5. Phase Diagram

Using the “Thermocalc” program (Powell and Holland, 1995) and the calcsilicate mineral assemblages found in the study area (Table 1) a phase diagram was produced which plotted all possible stable reactions for different X_{CO_2} values and pressure of 4.5 kbars. Several relevant reactions were calculated:



Of all the samples studied Ink2 provides the best example of assemblages that allow the $T - X_{CO_2}$ path to be determined.

The suggested path for Ink2 is shown on the phase diagram. The diagram was calculated at 4.5 kbar, based on hornblende geobarometry (Johnson and Rutherford, 1989) performed on sample Ink8 a hornblende bearing granodiorite. It is assumed that this granodiorite vein intruded close to the

metamorphic peak, and that the little metamorphic modification of the hornblende occurred in the D₃ and D₄ events. It is evident that the assemblages in calcsilicate rocks, such as Ink2, show equilibrium at low XCO₂ so are clearly fluid buffered.

In sample Ink2, garnet core contain only diopside (no wollastonite or vesuvianite). Reaction (1) defines diopside stability, whereas reaction (2) defines grossularite garnet stability. It is therefore postulated that the garnet core grew in the field (a), between reactions (2) and (3). The outer rims of the garnet porphyroblasts contain vesuvianite and wollastonite (Figures 5.1. and 5.2., chapter five) so that the reaction (7) must have been crossed and the rim must have formed at very low XCO₂ conditions (less than 0.05) and temperatures around 630° - 680° C, field (b) on Figure 5.15. In other samples, garnet coexists with quartz indicating reaction (5) was not crossed. The matrix of Ink2, however, contains abundant wollastonite and diopside, with no vesuvianite, indicating that it must have equilibrated at higher XCO₂ conditions relative to reactions (6) and (7), around (c) on Figure 5.15.

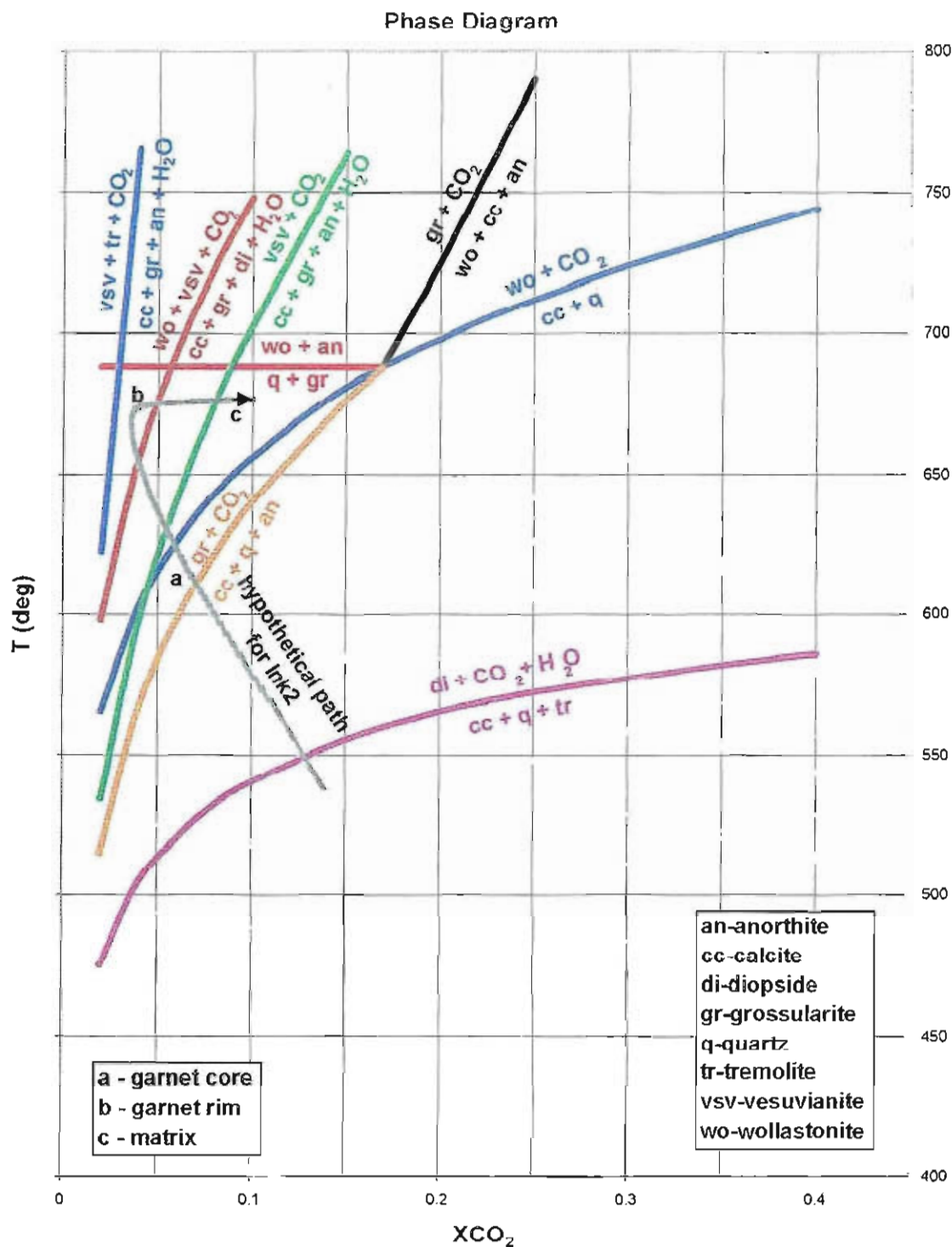


Figure 5.15. $T - X_{CO_2}$ plot obtained using Thermocalc, at 4.5 kbar. Assemblages in calcsilicate rocks such as InK2 show equilibrium at low X_{CO_2} so are clearly fluid buffered. The suggested path for InK2 is given.

Chapter Six

Discussion and Conclusions

6.1. Introduction

The metamorphosed rocks found in the study area are considered originally to be carbonate rich sediments and felsic igneous intrusions. The rocks were subjected to multiple deformation and metamorphism, and have also undergone metasomatism resulting in skarn development. A strong foliation is developed in all lithologies except for younger mafic dykes.

6.2. Geological History

The most common foliation fabric that can be noted in the Inkerman Metamorphics has been termed S_2 and the evidence of D_1 deformation event can be only seen in fold hinges of calcsilicates.

The second deformation event D_2 was marked by intrusion of granite veins and development of strong S_2 foliation forming characteristic gneissic layering. The peak metamorphic conditions were obtained at 4.5 kbar and at temperatures up to 650° C. Many granitic veins contain clinopyroxene and anorthite rich plagioclase, up to An_{90} , so it is postulated that metasomatic conditions resulted in the conversion of granite veins to endoskarn. The metasomatic process involved addition of Ca and probably removal of alkalies (Na, K). Therefore most of the endoskarn veins are composed of Ca rich plagioclase and with little or no K-feldspar. These pegmatitic veins are late D_2 or post D_2 .

The third deformation event D_3 can be noted in calcsilicate outcrops of the study area. This event is represented by shallowly dipping axial planes of S_3 .

The fourth deformation event D_4 is developed in monzogranite and syenogranite as a weak steeply dipping foliation. Therefore, the granitoids of the study area are intruded pre D_4 or alternatively intruded late in D_2 . In the calcsilicate rocks and gneiss D_4 is manifested as scattered folds with steep axial planes.

Mafic dykes that intruded all other lithologies show no evidence of foliation. These dykes are correlated with the Permo-Carboniferous mafic dyke swarm and postdates the development of the east-west foliation found in D_3 .

Ages of these deformation events are uncertain. Correlatives may be found in metamorphic rocks of Harvey's Range and are likely to be Proterozoic to Lower Palaeozoic. The peak metamorphism of the Harvey's Range rocks was syn- D_3 (Edison, 1995) and S_3 related to this event may be correlated to S_2 found in the Inkerman Metamorphics as both are of similar orientation (E-W). The S_3 at Harvey Range is probably Lower Palaeozoic in age, as it is developed in Ordovician Granodiorite (SHRIMP age, R. Henderson personal comm.; Rubenach, 1998). If the correlation is correct, that would make S_2 in Inkerman Shear Zone Lower Palaeozoic. However, the depositional age of the calcsilicates rocks is still uncertain.

6.3. Origin of the Calcsilicates and Skarns

Using "Thermocalc" program a phase diagram was constructed, using eight relevant reactions. Assemblages in samples such as Ink2 (garnet, wollastonite) indicate fluid buffering by low X_{CO_2} fluids. As abundant granite veins were injected close to the metamorphic peak, it is assumed that such fluids were of

magmatic origin. The pressure of 4.5 kbar suggests that the metamorphism occurred too deep for meteoric fluids to be involved.

6.3.1. calcsilicate reactions

Eight relevant stable reactions for calcsilicate mineral assemblages were calculated. During the reactions 1 to 5, where no vesuvianite was found in the mineral assemblage, the peak metamorphic temperature would have been between 650° C to 680° C. The calcsilicate assemblage in Ink2 was buffered approximately at 0.05% XCO₂.

6.3.2. skarn formation

The skarn development can be observed in garnet pods revealed in layered calcsilicates and conversion of granitic veins to endoskarn.

- a) Skarn formation can be observed in pods of andradite-rich garnets cropping out amongst layered calcsilicates where otherwise diopside dominated and garnet was a minor component. It was indicated that the fluid movement was not homogenous between the layers. These garnet pods may have been related to the localised fluid movement.
- b) The metasomatic process of introduction of Ca rich fluids at the same time prevailed the removal of alkalies (Na, K) from the granitic veins in gneiss. The Ca most likely was derived from calcsilicate or skarn alteration of adjacent marble or calcite-bearing calcsilicate rocks.

It is unclear if typical calcite-wollastonite-calcsilicate rocks are skarns too. It could only be determined if isotope studies were conducted but that is beyond the scope of the thesis.

6.4. Future Work

The Inkerman Metamorphics are a significant area of high-grade metamorphic rocks in the Stokes Range area. As the age of these metamorphic rocks is uncertain it is essential to suggest SHRIMP dating on zircon from various granites and endoskarn. This investigation would also help to determine the relationship between the granitoids found in this area and those of the Ravenswood Batholith.

To determine the origin of the fluids that caused the skarn development a stable isotope study (oxygen, carbon and hydrogen isotopes) should be conducted.

Reference List

- Barton M.D., Ilchik R.P. and Marikos M.A. (1991), *Metasomatism – Chapter 7, Contact Metamorphism* edited by Kerrick D.M. Published by Mineralogical Society of America, Volume 10, p. 321-350.
- Beams S.D. (1995), 17th IGES Exploring the Tropics, Townsville, Australia; *Mineral Deposits of Northeast Queensland: Geology and Geochemistry*, edited by S.D.Beams, p. 1-3.
- Carruthers D.S. (1954), Vermiculite and Asbestos Occurrences, Home Hill District, *Queensland Government Mining Journal* 55, p. 64-65.
- Draper J.J. (1998), An Overview of Post-Mesoproterozoic Mineralization in Queensland, *AGSO Journal of Australian Geology & Geophysics*, Volume 17, p. 61-67.
- Edison K.A. (1995) *Contact Metamorphism and Hornfelsing of Pelitic Sediments, Harvey's Range Aureole, Townsville, North Queensland*, Honours Thesis, James Cook University, Townsville (unpublished).
- Einaudi M.T., Meinert L.D. and Newberry R.J. (1980), Skarn Deposits, *Economic Geology*, Seventy-Fifth Anniversary Volume edited by Skinner B.J., p.317-383.
- Evans P.A. (1991), High-grade Regional Metamorphic Rocks in the Lower Burdekin District, North Queensland, Volume 3 *Queensland Government Mining Journal*, p. 363-369.
- Foster D. (1994) Deformation and Metamorphism in the Inkerman Shear Zone, *Third Year Field Project*, James Cook University, Townsville (unpublished).
- Gregory C.M. (1969), Ayr, Queensland – 1:250 000 Geological Series, Bureau of Mineral Resources, Australia, *Explanatory Notes SE55-15*.
- Holland T.J. and Powell R. (1985), An Internally Consistent Thermodynamic Dataset with Uncertainties and Correlations, *Journal of Metamorphic geology*, 3, p. 343-370.
- Hutton L.J., Draper J.J., Rienks I.P., Withnall I.W. and Knutson J. (1997), Charters Towers Region – Chapter 6, North Queensland Geology, *AGSO Bulletin 240/Queensland Geology* 9, Compiled and edited by J.H.C. Bain and J.J. Draper, p. 165-200.
- Jamtveit B., Grorud H.F. and Bucher-Nurminen K. (1992), Contact Metamorphism of Layered Carbonate-Shale Sequences in the Oslo Rift: II. Migration of Isotopic and Reaction Fronts around Cooling Plutons, Earth and Planetary Science letters, *Elsevier Science Publishers B.V., Amsterdam*, p. 131-149.
- Jamtveit B. and Anderson T. (1993), Contact Metamorphism of Layered Shale-Carbonate Sequences in the Oslo Rift: III. The Nature of Skarn Forming Fluids, *Economic Geology*, Volume 88, p. 1830-1849.
- Jamtveit B., Dahlgren S. and Austrheim H (1997), High-Grade Contact Metamorphism of Calcareous Rocks from the Oslo Rift, Southern Norway, *American Mineralogist*, Volume 82, p. 1241-1254.

- Johnson M.C. and M.J. Rutherford (1989) Hornblende Geobarometry in Granitoids, *Journal of Petrology*, Volume 30, p 711-737.
- Kwak T.A.P. (1987), W-Sn Skarn Deposits and Related Metamorphic Skarns and Granitoids, Published by Elsevier Science Publishers B.V. Amsterdam, p. 150-182.
- Newberry R.J., Einaudi M.T. and Eastman H.S. (1991), Zoning and Genesis of the Darwin Pb-Zn-Ag Skarn Deposit, California: A Reinterpretation Based on New Data, *Economic Geology*, Volume 86, p. 960-969.
- Nisbet B. and Goulevitch J. (1970), Final Report on Area 7 (Inkerman) A to P 535M QLD, *Trans Australian Explorations*, CR 3342.
- Paine A.G.L., Gregory C.M. and Clarke D.E. (1970), Geology of the Ayr 1:250 000 Sheet area, *Bureau of Mineral Resources, Australia*, Report 128.
- Rubenach M.J. (1998), Igneous and Metamorphic Geology of the Harvey Range Area, Short Geological Field Trips, Townsville – Charters Towers, 14th Australian Geological Convention, Townsville, July 1998, p. 54-59.
- Stephenson P.J. (1990), Some Aspects of Dyke Emplacement and Characteristics in Townsville-Ingham District, Australia, in Parker A.J. Rickwood P.C. and Tucker D.H., Mafic Dykes and Emplacement Mechanisms, *A.A. Balkema, Rotterdam*, p. 125-133.
- Traves D.M. (1951), A Geological Reconnaissance of the Townsville Bowen Region, Northern Queensland, *Bureau of Mineral Resources, Australia*, Record 1951/25.
- Withnall I.W., Blake P.R., Crouch S.B.S., Tenison Woods K., Grimes K.G., Hayward M.A., Lam J.S., Garrad P. and Rees I.D. (1997), Geology of the Southern Part of the Anakie Inlier, Central Queensland. *Queensland Geology*, Published by the Department of Minerals and Energy, Volume 7, p. 45-66.
- Yardley B.W.D., *An Introduction to Metamorphic Petrology*, Longman Earth Science Series, Chapter five: Metamorphism of Marbles and Calcsilicate Rocks, p. 126-146.

Appendix 1
Microprobe Analysis for Selected Specimens

Table 2: Microprobe Analysis of Garnets from Selected Calcsilicates

Ink2 gf core		Ink2 gf edge ₁		Ink2 gf edge ₂		Ink10 gf 1	
<i>SiO</i> ₂	39.20	<i>SiO</i> ₂	39.30	<i>SiO</i> ₂	37.80	<i>SiO</i> ₂	39.60
<i>TiO</i> ₂	0.42	<i>TiO</i> ₂	0.69	<i>TiO</i> ₂	0.60	<i>TiO</i> ₂	0.32
<i>Al</i> ₂ <i>O</i> ₃	18.30	<i>Al</i> ₂ <i>O</i> ₃	17.70	<i>Al</i> ₂ <i>O</i> ₃	17.70	<i>Al</i> ₂ <i>O</i> ₃	18.95
<i>Fe</i> ₂ <i>O</i> ₃	6.05	<i>Fe</i> ₂ <i>O</i> ₃	7.45	<i>Fe</i> ₂ <i>O</i> ₃	5.12	<i>Fe</i> ₂ <i>O</i> ₃	5.46
<i>FeO</i>	0.00	<i>FeO</i>	0.00	<i>FeO</i>	0.00	<i>FeO</i>	0.00
<i>MnO</i>	0.70	<i>MnO</i>	0.53	<i>MnO</i>	0.70	<i>MnO</i>	0.60
<i>MgO</i>	0.51	<i>MgO</i>	0.38	<i>MgO</i>	0.68	<i>MgO</i>	0.50
<i>CaO</i>	36.20	<i>CaO</i>	36.20	<i>CaO</i>	35.50	<i>CaO</i>	36.20
<i>Na</i> ₂ <i>O</i>	0.30	<i>Na</i> ₂ <i>O</i>	0.00	<i>Na</i> ₂ <i>O</i>	0.00	<i>Na</i> ₂ <i>O</i>	0.04
<i>K</i> ₂ <i>O</i>	0.12	<i>K</i> ₂ <i>O</i>	0.06	<i>K</i> ₂ <i>O</i>	0.13	<i>K</i> ₂ <i>O</i>	0.04
<i>Cl</i>	0.00	<i>Cl</i>	0.00	<i>Cl</i>	0.07	<i>Cl</i>	0.00
<i>P</i> ₂ <i>O</i> ₅	0.00	<i>P</i> ₂ <i>O</i> ₅	0.00	<i>P</i> ₂ <i>O</i> ₅	0.11	<i>P</i> ₂ <i>O</i> ₅	0.07
<i>Cr</i> ₂ <i>O</i> ₃	0.00	<i>Cr</i> ₂ <i>O</i> ₃	0.00	<i>Cr</i> ₂ <i>O</i> ₃	0.00	<i>Cr</i> ₂ <i>O</i> ₃	0.03
<i>NiO</i>	0.00	<i>NiO</i>	0.00	<i>NiO</i>	0.00	<i>NiO</i>	0.00
Total	101.80	Total	102.31	Total	98.41	Total	101.81
No. Oxygens	24						
<i>Si</i>	5.928	<i>Si</i>	5.926	<i>Si</i>	5.917	<i>Si</i>	5.962
<i>Ti</i>	0.048	<i>Ti</i>	0.078	<i>Ti</i>	0.071	<i>Ti</i>	0.036
<i>Al</i>	3.261	<i>Al</i>	3.145	<i>Al</i>	3.265	<i>Al</i>	3.362
<i>Fe</i> ³⁺	0.688	<i>Fe</i> ³⁺	0.845	<i>Fe</i> ³⁺	0.603	<i>Fe</i> ³⁺	0.619
<i>Fe</i> ²⁺	0.000						
<i>Mn</i>	0.090	<i>Mn</i>	0.068	<i>Mn</i>	0.093	<i>Mn</i>	0.076
<i>Mg</i>	0.115	<i>Mg</i>	0.085	<i>Mg</i>	0.159	<i>Mg</i>	0.111
<i>Ca</i>	5.864	<i>Ca</i>	5.848	<i>Ca</i>	5.953	<i>Ca</i>	5.838
<i>Na</i>	0.088	<i>Na</i>	0.000	<i>Na</i>	0.000	<i>Na</i>	0.010
<i>K</i>	0.023	<i>K</i>	0.012	<i>K</i>	0.026	<i>K</i>	0.007
<i>Cl</i>	0.000	<i>Cl</i>	0.000	<i>Cl</i>	0.009	<i>Cl</i>	0.000
Total	16.105	Total	16.007	Total	16.096	Total	16.021
<i>Si</i>	5.93	<i>Si</i>	5.93	<i>Si</i>	5.92	<i>Si</i>	5.96
<i>Al</i> ^{iv}	0.07	<i>Al</i> ^{iv}	0.07	<i>Al</i> ^{iv}	0.08	<i>Al</i> ^{iv}	0.04
<i>Al</i> ^{vi}	3.19	<i>Al</i> ^{vi}	3.07	<i>Al</i> ^{vi}	3.18	<i>Al</i> ^{vi}	3.32
<i>Fe</i> ³⁺	0.69	<i>Fe</i> ³⁺	0.85	<i>Fe</i> ³⁺	0.60	<i>Fe</i> ³⁺	0.62
<i>Ti</i>	0.05	<i>Ti</i>	0.08	<i>Ti</i>	0.07	<i>Ti</i>	0.04
<i>Fe</i> ²⁺	0.00						
<i>Mn</i>	0.09	<i>Mn</i>	0.07	<i>Mn</i>	0.09	<i>Mn</i>	0.08
<i>Mg</i>	0.11	<i>Mg</i>	0.09	<i>Mg</i>	0.16	<i>Mg</i>	0.11
<i>Ca</i>	5.86	<i>Ca</i>	5.85	<i>Ca</i>	5.95	<i>Ca</i>	5.84
<i>Pyrope</i>	1.89	<i>Pyrope</i>	1.42	<i>Pyrope</i>	2.56	<i>Pyrope</i>	1.84
<i>Andradite</i>	17.54	<i>Andradite</i>	21.16	<i>Andradite</i>	15.64	<i>Andradite</i>	15.55
<i>Almandine</i>	0.00	<i>Almandine</i>	0.00	<i>Almandine</i>	0.00	<i>Almandine</i>	0.00
<i>Spessartine</i>	1.48	<i>Spessartine</i>	1.13	<i>Spessartine</i>	1.50	<i>Spessartine</i>	1.27
<i>Grossular</i>	79.09	<i>Grossular</i>	76.29	<i>Grossular</i>	80.30	<i>Grossular</i>	81.34
Total	100.00	Total	100.00	Total	100.00	Total	100.00

Table 2: Microprobe Analysis of Garnets from Selected Calcilicates (Cont.)

Ink13-p1-gt1	Ink13-p1-gt2	Ink13-p1-gt3	Ink13-p1-gt less Fe
<i>SiO</i> ₂ 38.90	<i>SiO</i> ₂ 38.50	<i>SiO</i> ₂ 38.20	<i>SiO</i> ₂ 39.00
<i>TiO</i> ₂ 0.64	<i>TiO</i> ₂ 0.19	<i>TiO</i> ₂ 0.28	<i>TiO</i> ₂ 0.02
<i>Al</i> ₂ <i>O</i> ₃ 14.40	<i>Al</i> ₂ <i>O</i> ₃ 15.20	<i>Al</i> ₂ <i>O</i> ₃ 13.00	<i>Al</i> ₂ <i>O</i> ₃ 25.20
<i>Fe</i> ₂ <i>O</i> ₃ 11.23	<i>Fe</i> ₂ <i>O</i> ₃ 9.7	<i>Fe</i> ₂ <i>O</i> ₃ 14.23	<i>Fe</i> ₂ <i>O</i> ₃ 9.51
<i>FeO</i> 0.00	<i>FeO</i> 0.00	<i>FeO</i> 0.00	<i>FeO</i> 0.00
<i>MnO</i> 0.53	<i>MnO</i> 0.65	<i>MnO</i> 1.10	<i>MnO</i> 0.06
<i>MgO</i> 0.17	<i>MgO</i> 0.02	<i>MgO</i> 0.02	<i>MgO</i> 0.05
<i>CaO</i> 33.70	<i>CaO</i> 34.00	<i>CaO</i> 31.00	<i>CaO</i> 22.70
<i>Na</i> ₂ <i>O</i> 0.11	<i>Na</i> ₂ <i>O</i> 0.01	<i>Na</i> ₂ <i>O</i> 0.06	<i>Na</i> ₂ <i>O</i> 0.08
<i>K</i> ₂ <i>O</i> 0.01	<i>K</i> ₂ <i>O</i> 0.08	<i>K</i> ₂ <i>O</i> 0.14	<i>K</i> ₂ <i>O</i> 0.12
<i>Cl</i> 0.01	<i>Cl</i> 0.01	<i>Cl</i> 0.01	<i>Cl</i> 0.00
<i>P</i> ₂ <i>O</i> ₅ 0.04	<i>P</i> ₂ <i>O</i> ₅ 0.00	<i>P</i> ₂ <i>O</i> ₅ 0.00	<i>P</i> ₂ <i>O</i> ₅ 0.00
<i>Cr</i> ₂ <i>O</i> ₃ 0.06	<i>Cr</i> ₂ <i>O</i> ₃ 0.00	<i>Cr</i> ₂ <i>O</i> ₃ 0.00	<i>Cr</i> ₂ <i>O</i> ₃ 0.00
<i>NiO</i> 0.00	<i>NiO</i> 0.00	<i>NiO</i> 0.00	<i>NiO</i> 0.00
Total 99.80	Total 98.36	Total 98.04	Total 96.74
No. Oxygens 24	No. Oxygens 24	No. Oxygens 24	No. Oxygens 24
<i>Si</i> 6.070	<i>Si</i> 6.072	<i>Si</i> 6.105	<i>Si</i> 5.927
<i>Ti</i> 0.075	<i>Ti</i> 0.023	<i>Ti</i> 0.034	<i>Ti</i> 0.002
<i>Al</i> 2.648	<i>Al</i> 2.825	<i>Al</i> 2.448	<i>Al</i> 4.514
<i>Fe</i> ³⁺ 1.318	<i>Fe</i> ³⁺ 1.151	<i>Fe</i> ³⁺ 1.711	<i>Fe</i> ³⁺ 1.088
<i>Fe</i> ²⁺ 0.000	<i>Fe</i> ²⁺ 0.000	<i>Fe</i> ²⁺ 0.000	<i>Fe</i> ²⁺ 0.000
<i>Mn</i> 0.070	<i>Mn</i> 0.087	<i>Mn</i> 0.149	<i>Mn</i> 0.008
<i>Mg</i> 0.040	<i>Mg</i> 0.005	<i>Mg</i> 0.005	<i>Mg</i> 0.011
<i>Ca</i> 5.633	<i>Ca</i> 5.745	<i>Ca</i> 5.307	<i>Ca</i> 3.696
<i>Na</i> 0.033	<i>Na</i> 0.003	<i>Na</i> 0.019	<i>Na</i> 0.024
<i>K</i> 0.002	<i>K</i> 0.016	<i>K</i> 0.029	<i>K</i> 0.023
<i>Cl</i> 0.001	<i>Cl</i> 0.001	<i>Cl</i> 0.000	<i>Cl</i> 0.000
Total 15.890	Total 15.928	Total 15.807	Total 15.293
<i>Si</i> 6.07	<i>Si</i> 6.07	<i>Si</i> 6.10	<i>Si</i> 5.93
<i>Al</i> ^{iv} -0.07	<i>Al</i> ^{iv} -0.07	<i>Al</i> ^{iv} -0.10	<i>Al</i> ^{iv} 0.07
<i>Al</i> ^{vi} 2.72	<i>Al</i> ^{vi} 2.90	<i>Al</i> ^{vi} 2.55	<i>Al</i> ^{vi} 4.44
<i>Fe</i> ³⁺ 1.32	<i>Fe</i> ³⁺ 1.15	<i>Fe</i> ³⁺ 1.71	<i>Fe</i> ³⁺ 1.09
<i>Ti</i> 0.08	<i>Ti</i> 0.02	<i>Ti</i> 0.03	<i>Ti</i> 0.00
<i>Fe</i> ²⁺ 0.00	<i>Fe</i> ²⁺ 0.00	<i>Fe</i> ²⁺ 0.00	<i>Fe</i> ²⁺ 0.00
<i>Mn</i> 0.07	<i>Mn</i> 0.09	<i>Mn</i> 0.15	<i>Mn</i> 0.01
<i>Mg</i> 0.04	<i>Mg</i> 0.04	<i>Mg</i> 0.00	<i>Mg</i> 0.01
<i>Ca</i> 5.63	<i>Ca</i> 5.74	<i>Ca</i> 5.31	<i>Ca</i> 3.70
<i>Pyrope</i> 0.69	<i>Pyrope</i> 0.08	<i>Pyrope</i> 0.08	<i>Pyrope</i> 0.30
<i>Andradite</i> 32.07	<i>Andradite</i> 28.28	<i>Andradite</i> 39.82	<i>Andradite</i> 19.67
<i>Almandine</i> 0.00	<i>Almandine</i> 0.00	<i>Almandine</i> 0.00	<i>Almandine</i> 0.00
<i>Spessartine</i> 1.22	<i>Spessartine</i> 1.49	<i>Spessartine</i> 2.73	<i>Spessartine</i> 0.21
<i>Grossular</i> 66.02	<i>Grossular</i> 70.15	<i>Grossular</i> 57.37	<i>Grossular</i> 79.82
Total 100.00	Total 100.00	Total 100.00	Total 100.00

Table 3 Microprobe Analysis of Clinopyroxene for Selected Specimens

<i>Ink15 cpx1</i>		<i>Ink15 cpx2</i>		<i>Ink13 cpx2</i>		<i>Ink7 cpx</i>	
<i>Oxide</i>	<i>Weight %</i>						
<i>SiO₂</i>	51.00	<i>SiO₂</i>	50.20	<i>SiO₂</i>	53.80	<i>SiO₂</i>	52.95
<i>TiO₂</i>	0.00	<i>TiO₂</i>	0.00	<i>TiO₂</i>	0.23	<i>TiO₂</i>	0.35
<i>Al₂O₃</i>	1.41	<i>Al₂O₃</i>	0.98	<i>Al₂O₃</i>	0.60	<i>Al₂O₃</i>	1.78
<i>Fe₂O₃</i>	0.00	<i>Fe₂O₃</i>	0.00	<i>Fe₂O₃</i>	10.40	<i>Fe₂O₃</i>	0.00
<i>FeO</i>	15.70	<i>FeO</i>	14.30	<i>FeO</i>	0.00	<i>FeO</i>	8.28
<i>MnO</i>	0.96	<i>MnO</i>	1.01	<i>MnO</i>	0.63	<i>MnO</i>	0.40
<i>MgO</i>	8.06	<i>MgO</i>	8.53	<i>MgO</i>	11.60	<i>MgO</i>	12.75
<i>CaO</i>	23.60	<i>CaO</i>	23.50	<i>CaO</i>	24.60	<i>CaO</i>	23.90
<i>Na₂O</i>	0.00	<i>Na₂O</i>	0.94	<i>Na₂O</i>	0.26	<i>Na₂O</i>	0.43
<i>K₂O</i>	0.00	<i>K₂O</i>	0.12	<i>K₂O</i>	0.07	<i>K₂O</i>	0.06
<i>Cl</i>	0.00	<i>Cl</i>	0.03	<i>Cl</i>	0.07	<i>Cl</i>	0.01
<i>P₂O₅</i>	0.00	<i>P₂O₅</i>	0.00	<i>P₂O₅</i>	0.00	<i>P₂O₅</i>	0.00
<i>Cr₂O₃</i>	0.06	<i>Cr₂O₃</i>	0.00	<i>Cr₂O₃</i>	0.00	<i>Cr₂O₃</i>	0.06
<i>NiO</i>	0.00	<i>NiO</i>	0.00	<i>NiO</i>	0.00	<i>NiO</i>	0.02
Total	100.73	Total	99.61	Total	102.24	Total	100.90
<i>No of Oxygens 6</i>		<i>No of Oxygens 6</i>		<i>No of Oxygens 6</i>		<i>No of Oxygens 6</i>	
<i>Si</i>	1.965	<i>Si</i>	1.958	<i>Si</i>	1.953	<i>Si</i>	1.962
<i>Ti</i>	0.000	<i>Ti</i>	0.000	<i>Ti</i>	0.006	<i>Ti</i>	0.010
<i>Al</i>	0.064	<i>Al</i>	0.045	<i>Al</i>	0.026	<i>Al</i>	0.078
<i>Fe³⁺</i>	0.000	<i>Fe³⁺</i>	0.000	<i>Fe³⁺</i>	0.284	<i>Fe³⁺</i>	0.000
<i>Fe²⁺</i>	0.506	<i>Fe²⁺</i>	0.466	<i>Fe²⁺</i>	0.000	<i>Fe²⁺</i>	0.257
<i>Mn</i>	0.031	<i>Mn</i>	0.033	<i>Mn</i>	0.019	<i>Mn</i>	0.013
<i>Mg</i>	0.463	<i>Mg</i>	0.496	<i>Mg</i>	0.628	<i>Mg</i>	0.704
<i>Ca</i>	0.974	<i>Ca</i>	0.982	<i>Ca</i>	0.957	<i>Ca</i>	0.949
<i>Na</i>	0.000	<i>Na</i>	0.071	<i>Na</i>	0.018	<i>Na</i>	0.031
<i>K</i>	0.000	<i>K</i>	0.006	<i>K</i>	0.003	<i>K</i>	0.003
<i>Cl</i>	0.000	<i>Cl</i>	0.001	<i>Cl</i>	0.002	<i>Cl</i>	0.000
Total	4.003	Total	4.059	Total	3.897	Total	4.006
<i>Fe No*</i>	27.207	<i>Fe No*</i>	25.267	<i>Fe No*</i>	16.073	<i>Fe No*</i>	14.000
<i>Mg No*</i>	23.450	<i>Mg No*</i>	25.086	<i>Mg No*</i>	33.252	<i>Mg No*</i>	36.642
<i>Ca No*</i>	49.342	<i>Ca No*</i>	49.647	<i>Ca No*</i>	50.675	<i>Ca No*</i>	49.358
Total	100.000	Total	100.000	Total	100.000	Total	100.000

Table 4 Microprobe Analysis of Diopside for Selected Calcsilicates

Ink2 diop 1		Ink2 diop incl near gt edge		Ink2 diop in gt core	
<i>Oxide</i>	<i>Weight %</i>	<i>Oxide</i>	<i>Weight %</i>	<i>Oxide</i>	<i>Weight %</i>
<i>SiO</i> ₂	53.80	<i>SiO</i> ₂	53.90	<i>SiO</i> ₂	52.70
<i>TiO</i> ₂	0.05	<i>TiO</i> ₂	0.16	<i>TiO</i> ₂	0.30
<i>Al</i> ₂ <i>O</i> ₃	2.00	<i>Al</i> ₂ <i>O</i> ₃	1.58	<i>Al</i> ₂ <i>O</i> ₃	1.57
<i>Fe</i> ₂ <i>O</i> ₃	0.00	<i>Fe</i> ₂ <i>O</i> ₃	0.00	<i>Fe</i> ₂ <i>O</i> ₃	0.00
<i>FeO</i>	6.81	<i>FeO</i>	7.21	<i>FeO</i>	8.12
<i>MnO</i>	0.56	<i>MnO</i>	0.72	<i>MnO</i>	0.44
<i>MgO</i>	12.20	<i>MgO</i>	11.90	<i>MgO</i>	12.40
<i>CaO</i>	26.10	<i>CaO</i>	25.40	<i>CaO</i>	25.20
<i>Na</i> ₂ <i>O</i>	0.00	<i>Na</i> ₂ <i>O</i>	0.49	<i>Na</i> ₂ <i>O</i>	0.21
<i>K</i> ₂ <i>O</i>	0.00	<i>K</i> ₂ <i>O</i>	0.01	<i>K</i> ₂ <i>O</i>	0.06
<i>Cl</i>	0.05	<i>Cl</i>	0.00	<i>Cl</i>	0.05
<i>P</i> ₂ <i>O</i> ₅	0.04	<i>P</i> ₂ <i>O</i> ₅	0.30	<i>P</i> ₂ <i>O</i> ₅	0.00
<i>Cr</i> ₂ <i>O</i> ₃	0.00	<i>Cr</i> ₂ <i>O</i> ₃	0.01	<i>Cr</i> ₂ <i>O</i> ₃	0.00
<i>NiO</i>	0.00	<i>NiO</i>	0.00	<i>NiO</i>	0.08
<i>Total</i>	101.61	<i>Total</i>	101.68	<i>Total</i>	101.13
<i>No of Oxygens 6</i>		<i>No of Oxygens 6</i>		<i>No of Oxygens 6</i>	
<i>Si</i>	1.974	<i>Si</i>	1.985	<i>Si</i>	1.982
<i>Ti</i>	0.001	<i>Ti</i>	0.004	<i>Ti</i>	0.005
<i>Al</i>	0.086	<i>Al</i>	0.069	<i>Al</i>	0.054
<i>Fe</i> ³⁺	0.000	<i>Fe</i> ³⁺	0.000	<i>Fe</i> ³⁺	0.000
<i>Fe</i> ²⁺	0.209	<i>Fe</i> ²⁺	0.222	<i>Fe</i> ²⁺	0.203
<i>Mn</i>	0.017	<i>Mn</i>	0.022	<i>Mn</i>	0.009
<i>Mg</i>	0.667	<i>Mg</i>	0.653	<i>Mg</i>	0.721
<i>Ca</i>	1.026	<i>Ca</i>	1.002	<i>Ca</i>	0.993
<i>Na</i>	0.000	<i>Na</i>	0.035	<i>Na</i>	0.040
<i>K</i>	0.000	<i>K</i>	0.000	<i>K</i>	0.000
<i>Cl</i>	0.002	<i>Cl</i>	0.000	<i>Cl</i>	0.000
<i>Total</i>	3.982	<i>Total</i>	3.994	<i>Total</i>	4.006
<i>Fe No*</i>	11.79	<i>Fe No*</i>	12.87	<i>Fe No*</i>	13.60
<i>Mg No*</i>	34.76	<i>Mg No*</i>	34.39	<i>Mg No*</i>	35.11
<i>Ca No*</i>	53.45	<i>Ca No*</i>	52.74	<i>Ca No*</i>	51.28
<i>Total</i>	100.00	<i>Total</i>	100.00	<i>Total</i>	100.00
<i>Fe = (Fe³⁺ + Fe²⁺ + Mn)</i>					

Table 4 Microprobe Analysis of Diopside for Selected Calcsilicates (Cont.)

lnk10 diop in matrix		lnk10 p2 diop1		lnk13 p2 diop2	
<i>Oxide</i>	<i>Weight %</i>	<i>Oxide</i>	<i>Weight %</i>	<i>Oxide</i>	<i>Weight %</i>
<i>SiO₂</i>	54.10	<i>SiO₂</i>	50.50	<i>SiO₂</i>	50.60
<i>TiO₂</i>	0.17	<i>TiO₂</i>	0.08	<i>TiO₂</i>	0.12
<i>Al₂O₃</i>	1.25	<i>Al₂O₃</i>	1.51	<i>Al₂O₃</i>	1.61
<i>Fe₂O₃</i>	0.00	<i>Fe₂O₃</i>	0.00	<i>Fe₂O₃</i>	0.00
<i>FeO</i>	6.63	<i>FeO</i>	16.30	<i>FeO</i>	16.20
<i>MnO</i>	0.28	<i>MnO</i>	0.58	<i>MnO</i>	0.79
<i>MgO</i>	13.20	<i>MgO</i>	7.49	<i>MgO</i>	7.75
<i>CaO</i>	25.30	<i>CaO</i>	23.40	<i>CaO</i>	23.60
<i>Na₂O</i>	0.56	<i>Na₂O</i>	0.00	<i>Na₂O</i>	0.50
<i>K₂O</i>	0.00	<i>K₂O</i>	0.02	<i>K₂O</i>	0.10
<i>Cl</i>	0.00	<i>Cl</i>	0.00	<i>Cl</i>	0.06
<i>P₂O₅</i>	0.06	<i>P₂O₅</i>	0.00	<i>P₂O₅</i>	0.00
<i>Cr₂O₃</i>	0.13	<i>Cr₂O₃</i>	0.03	<i>Cr₂O₃</i>	0.00
<i>NiO</i>	0.00	<i>NiO</i>	0.00	<i>NiO</i>	0.00
Total	101.68	Total	99.91	Total	101.33
<i>No of Oxygens 6</i>		<i>No of Oxygens 6</i>		<i>No of Oxygens 6</i>	
<i>Si</i>	1.982	<i>Si</i>	1.966	<i>Si</i>	1.948
<i>Ti</i>	0.005	<i>Ti</i>	0.002	<i>Ti</i>	0.003
<i>Al</i>	0.054	<i>Al</i>	0.069	<i>Al</i>	0.073
<i>Fe³⁺</i>	0.000	<i>Fe³⁺</i>	0.000	<i>Fe³⁺</i>	0.000
<i>Fe²⁺</i>	0.203	<i>Fe²⁺</i>	0.530	<i>Fe²⁺</i>	0.522
<i>Mn</i>	0.009	<i>Mn</i>	0.019	<i>Mn</i>	0.026
<i>Mg</i>	0.721	<i>Mg</i>	0.435	<i>Mg</i>	0.445
<i>Ca</i>	0.993	<i>Ca</i>	0.976	<i>Ca</i>	0.973
<i>Na</i>	0.040	<i>Na</i>	0.000	<i>Na</i>	0.037
<i>K</i>	0.000	<i>K</i>	0.001	<i>K</i>	0.005
<i>Cl</i>	0.000	<i>Cl</i>	0.000	<i>Cl</i>	0.002
Total	4.006	Total	3.998	Total	4.034
<i>Fe No*</i>	11.00	<i>Fe No*</i>	28.04	<i>Fe No*</i>	27.84
<i>Mg No*</i>	37.44	<i>Mg No*</i>	22.17	<i>Mg No*</i>	22.63
<i>Ca No*</i>	51.56	<i>Ca No*</i>	49.78	<i>Ca No*</i>	49.52
Total	100.00	Total	100.00	Total	100.00
Fe = (Fe³⁺ + Fe²⁺ + Mn)					

Table 5 Microprobe Analysis of Plagioclase for Selected Specimens

<i>Ink15 plag centre</i>		<i>Ink15 plag 1/2 way</i>		<i>Ink8 plag centre</i>		<i>Ink8 plag edge</i>		<i>Ink8 p2 plag core</i>	
<i>Oxide</i>	<i>Weight %</i>								
<i>SiO₂</i>	45.40	<i>SiO₂</i>	45.40	<i>SiO₂</i>	55.20	<i>SiO₂</i>	56.05	<i>SiO₂</i>	55.50
<i>TiO₂</i>	0.07	<i>TiO₂</i>	0.10	<i>TiO₂</i>	0.01	<i>TiO₂</i>	0.35	<i>TiO₂</i>	0.20
<i>Al₂O₃</i>	34.10	<i>Al₂O₃</i>	33.80	<i>Al₂O₃</i>	28.85	<i>Al₂O₃</i>	27.75	<i>Al₂O₃</i>	29.00
<i>Fe₂O₃</i>	0.00								
<i>FeO</i>	0.14	<i>FeO</i>	0.22	<i>FeO</i>	0.23	<i>FeO</i>	0.30	<i>FeO</i>	0.12
<i>MnO</i>	0.85	<i>MnO</i>	0.85	<i>MnO</i>	0.04	<i>MnO</i>	0.03	<i>MnO</i>	0.04
<i>MgO</i>	1.50	<i>MgO</i>	1.48	<i>MgO</i>	0.64	<i>MgO</i>	0.27	<i>MgO</i>	0.65
<i>CaO</i>	18.50	<i>CaO</i>	18.30	<i>CaO</i>	11.80	<i>CaO</i>	11.45	<i>CaO</i>	10.80
<i>Na₂O</i>	1.85	<i>Na₂O</i>	1.33	<i>Na₂O</i>	1.50	<i>Na₂O</i>	5.32	<i>Na₂O</i>	4.95
<i>K₂O</i>	0.01	<i>K₂O</i>	0.15	<i>K₂O</i>	0.03	<i>K₂O</i>	0.23	<i>K₂O</i>	0.24
<i>Cl</i>	0.05	<i>Cl</i>	0.01	<i>Cl</i>	0.01	<i>Cl</i>	0.05	<i>Cl</i>	0.01
<i>P₂O₅</i>	0.00								
<i>Cr₂O₃</i>	0.04	<i>Cr₂O₃</i>	0.00	<i>Cr₂O₃</i>	0.00	<i>Cr₂O₃</i>	0.00	<i>Cr₂O₃</i>	0.00
<i>NiO</i>	0.00								
<i>Total</i>	102.51	<i>Total</i>	101.64	<i>Total</i>	98.31	<i>Total</i>	101.80	<i>Total</i>	101.51
<i>No of Oxygens 32</i>		<i>No of Oxygens 32</i>		<i>No of Oxygens 32</i>		<i>No of Oxygens 32</i>		<i>No of Oxygens 32</i>	
<i>Si</i>	8.259	<i>Si</i>	8.311	<i>Si</i>	9.996	<i>Si</i>	9.967	<i>Si</i>	9.856
<i>Ti</i>	0.010	<i>Ti</i>	0.014	<i>Ti</i>	0.001	<i>Ti</i>	0.047	<i>Ti</i>	0.027
<i>Al</i>	7.311	<i>Al</i>	7.292	<i>Al</i>	6.157	<i>Al</i>	5.816	<i>Al</i>	6.069
<i>Fe³⁺</i>	0.000								
<i>Fe²⁺</i>	0.021	<i>Fe²⁺</i>	0.034	<i>Fe²⁺</i>	0.034	<i>Fe²⁺</i>	0.045	<i>Fe²⁺</i>	0.018
<i>Mn</i>	0.130	<i>Mn</i>	0.132	<i>Mn</i>	0.005	<i>Mn</i>	0.004	<i>Mn</i>	0.006
<i>Mg</i>	0.407	<i>Mg</i>	0.404	<i>Mg</i>	0.173	<i>Mg</i>	0.072	<i>Mg</i>	0.172
<i>Ca</i>	3.605	<i>Ca</i>	3.589	<i>Ca</i>	2.289	<i>Ca</i>	2.181	<i>Ca</i>	2.055
<i>Na</i>	0.651	<i>Na</i>	0.472	<i>Na</i>	0.527	<i>Na</i>	1.834	<i>Na</i>	1.704
<i>K</i>	0.002	<i>K</i>	0.034	<i>K</i>	0.008	<i>K</i>	0.051	<i>K</i>	0.053
<i>Cl</i>	0.007	<i>Cl</i>	0.002	<i>Cl</i>	0.002	<i>Cl</i>	0.007	<i>Cl</i>	0.002
<i>P</i>	0.000								
<i>Cr</i>	0.004	<i>Cr</i>	0.000	<i>Cr</i>	0.000	<i>Cr</i>	0.000	<i>Cr</i>	0.000
<i>Ni</i>	0.000								
<i>Total</i>	20.407	<i>Total</i>	20.284	<i>Total</i>	19.192	<i>Total</i>	20.024	<i>Total</i>	19.962
<i>Anorthite (An)</i>	84.63	<i>Anorthite (An)</i>	87.62	<i>Anorthite (An)</i>	81.07	<i>Anorthite (An)</i>	53.63	<i>Anorthite (An)</i>	53.90
<i>Albite (Ab)</i>	15.32	<i>Albite (Ab)</i>	11.52	<i>Albite (Ab)</i>	18.65	<i>Albite (Ab)</i>	45.09	<i>Albite (Ab)</i>	44.70
<i>K-feldspar (Or)</i>	0.05	<i>K-feldspar (Or)</i>	0.86	<i>K-feldspar (Or)</i>	0.28	<i>K-feldspar (Or)</i>	1.28	<i>K-feldspar (Or)</i>	1.40
<i>Total</i>	100.00								

Table 5 Microprobe Analysis of Plagioclase for Selected Specimens (Cont.)

<i>Ink13 p2 plag1</i>		<i>Ink13 p2 plag rim</i>		<i>Ink13 p4 plag1</i>		<i>Ink7 p1 plag1</i>	
Oxide	Weight %						
<i>SiO₂</i>	47.35	<i>SiO₂</i>	46.90	<i>SiO₂</i>	58.80	<i>SiO₂</i>	57.20
<i>TiO₂</i>	0.09	<i>TiO₂</i>	0.07	<i>TiO₂</i>	0.01	<i>TiO₂</i>	0.01
<i>Al₂O₃</i>	33.85	<i>Al₂O₃</i>	33.30	<i>Al₂O₃</i>	26.05	<i>Al₂O₃</i>	26.85
<i>Fe₂O₃</i>	0.00	<i>Fe₂O₃</i>	0.00	<i>Fe₂O₃</i>	0.00	<i>Fe₂O₃</i>	0.00
<i>FeO</i>	0.23	<i>FeO</i>	0.43	<i>FeO</i>	0.09	<i>FeO</i>	0.45
<i>MnO</i>	0.12	<i>MnO</i>	0.01	<i>MnO</i>	0.01	<i>MnO</i>	0.04
<i>MgO</i>	0.01	<i>MgO</i>	0.01	<i>MgO</i>	0.01	<i>MgO</i>	0.01
<i>CaO</i>	18.60	<i>CaO</i>	18.30	<i>CaO</i>	8.81	<i>CaO</i>	9.68
<i>Na₂O</i>	1.14	<i>Na₂O</i>	1.03	<i>Na₂O</i>	6.35	<i>Na₂O</i>	6.02
<i>K₂O</i>	0.01	<i>K₂O</i>	0.19	<i>K₂O</i>	0.28	<i>K₂O</i>	0.25
<i>Cl</i>	0.01	<i>Cl</i>	0.01	<i>Cl</i>	0.03	<i>Cl</i>	0.00
<i>P₂O₅</i>	0.00	<i>P₂O₅</i>	0.00	<i>P₂O₅</i>	0.00	<i>P₂O₅</i>	0.00
<i>Cr₂O₃</i>	0.23	<i>Cr₂O₃</i>	0.05	<i>Cr₂O₃</i>	0.03	<i>Cr₂O₃</i>	0.03
<i>NiO</i>	0.00	<i>NiO</i>	0.11	<i>NiO</i>	0.37	<i>NiO</i>	0.31
Total	101.64	Total	100.41	Total	100.84	Total	100.85
<i>No of Oxygens 32</i>		<i>No of Oxygens 32</i>		<i>No of Oxygens 32</i>		<i>No of Oxygens 32</i>	
<i>Si</i>	8.605	<i>Si</i>	8.631	<i>Si</i>	10.465	<i>Si</i>	10.173
<i>Ti</i>	0.012	<i>Ti</i>	0.010	<i>Ti</i>	0.001	<i>Ti</i>	0.001
<i>Al</i>	7.055	<i>Al</i>	7.220	<i>Al</i>	5.472	<i>Al</i>	5.667
<i>Fe³⁺</i>	0.000	<i>Fe³⁺</i>	0.000	<i>Fe³⁺</i>	0.000	<i>Fe³⁺</i>	0.000
<i>Fe²⁺</i>	0.034	<i>Fe²⁺</i>	0.063	<i>Fe²⁺</i>	0.013	<i>Fe²⁺</i>	0.067
<i>Mn</i>	0.018	<i>Mn</i>	0.002	<i>Mn</i>	0.002	<i>Mn</i>	0.006
<i>Mg</i>	0.003	<i>Mg</i>	0.003	<i>Mg</i>	0.003	<i>Mg</i>	0.003
<i>Ca</i>	3.623	<i>Ca</i>	3.608	<i>Ca</i>	1.682	<i>Ca</i>	1.757
<i>Na</i>	0.402	<i>Na</i>	0.367	<i>Na</i>	2.094	<i>Na</i>	2.089
<i>K</i>	0.001	<i>K</i>	0.045	<i>K</i>	0.064	<i>K</i>	0.056
<i>Cl</i>	0.001	<i>Cl</i>	0.010	<i>Cl</i>	0.004	<i>Cl</i>	0.000
<i>P</i>	0.000	<i>P</i>	0.000	<i>P</i>	0.000	<i>P</i>	0.000
<i>Cr</i>	0.201	<i>Cr</i>	0.007	<i>Cr</i>	0.011	<i>Cr</i>	0.010
<i>Ni</i>	0.000	<i>Ni</i>	0.013	<i>Ni</i>	0.175	<i>Ni</i>	0.165
Total	19.955	Total	19.979	Total	19.986	Total	19.994
<i>Anorthite (An)</i>	89.99	<i>Anorthite (An)</i>	89.75	<i>Anorthite (An)</i>	42.70	<i>Anorthite (An)</i>	46.40
<i>Albite (Ab)</i>	9.98	<i>Albite (Ab)</i>	9.14	<i>Albite (Ab)</i>	55.68	<i>Albite (Ab)</i>	52.19
<i>K-feldspar (Or)</i>	0.03	<i>K-feldspar (Or)</i>	1.11	<i>K-feldspar (Or)</i>	1.62	<i>K-feldspar (Or)</i>	1.41
Total	100.00	Total	100.00	Total	100.00	Total	100.00

Table 6 Microprobe Analysis of Epidote for Selected Specimens

<i>Ink15 pl epid</i>		<i>Ink15 pl epid3</i>		<i>Ink/ epid</i>	
<i>Oxide</i>	<i>Weight %</i>	<i>Oxide</i>	<i>Weight %</i>	<i>Oxide</i>	<i>Weight %</i>
<i>SiO₂</i>	34.45	<i>SiO₂</i>	34.78	<i>SiO₂</i>	37.70
<i>TiO₂</i>	0.00	<i>TiO₂</i>	0.00	<i>TiO₂</i>	0.00
<i>Al₂O₃</i>	18.10	<i>Al₂O₃</i>	17.95	<i>Al₂O₃</i>	21.10
<i>Fe₂O₃</i>	16.56	<i>Fe₂O₃</i>	18.35	<i>Fe₂O₃</i>	15.78
<i>FeO</i>	0.00	<i>FeO</i>	0.00	<i>FeO</i>	0.00
<i>MnO</i>	0.43	<i>MnO</i>	0.13	<i>MnO</i>	0.12
<i>MgO</i>	0.98	<i>MgO</i>	0.72	<i>MgO</i>	0.05
<i>CaO</i>	18.70	<i>CaO</i>	17.70	<i>CaO</i>	23.50
<i>Na₂O</i>	0.78	<i>Na₂O</i>	0.35	<i>Na₂O</i>	0.06
<i>K₂O</i>	0.00	<i>K₂O</i>	0.00	<i>K₂O</i>	0.12
<i>Cl</i>	0.03	<i>Cl</i>	0.03	<i>Cl</i>	0.00
<i>P₂O₅</i>	0.00	<i>P₂O₅</i>	0.02	<i>P₂O₅</i>	0.00
<i>Cr₂O₃</i>	0.00	<i>Cr₂O₃</i>	0.00	<i>Cr₂O₃</i>	0.00
<i>NiO</i>	0.00	<i>NiO</i>	0.00	<i>NiO</i>	0.00
<i>Total</i>	90.03	<i>Total</i>	90.03	<i>Total</i>	98.43
<i>No of Oxygens 32</i>		<i>No of Oxygens 32</i>		<i>No of Oxygens 32</i>	
<i>Si</i>	7.752	<i>Si</i>	7.810	<i>Si</i>	7.733
<i>Ti</i>	0.000	<i>Ti</i>	0.000	<i>Ti</i>	0.000
<i>Al</i>	4.800	<i>Al</i>	4.750	<i>Al</i>	5.101
<i>Fe³⁺</i>	2.804	<i>Fe³⁺</i>	3.101	<i>Fe³⁺</i>	2.436
<i>Fe²⁺</i>	0.000	<i>Fe²⁺</i>	0.000	<i>Fe²⁺</i>	0.000
<i>Mn</i>	0.082	<i>Mn</i>	0.025	<i>Mn</i>	0.021
<i>Mg</i>	0.329	<i>Mg</i>	0.241	<i>Mg</i>	0.015
<i>Ca</i>	4.508	<i>Ca</i>	4.258	<i>Ca</i>	5.164
<i>Na</i>	0.340	<i>Na</i>	0.152	<i>Na</i>	0.024
<i>K</i>	0.000	<i>K</i>	0.000	<i>K</i>	0.031
<i>Cl</i>	0.004	<i>Cl</i>	0.006	<i>Cl</i>	0.000
<i>P</i>	0.000	<i>P</i>	0.040	<i>P</i>	0.000
<i>Cr</i>	0.000	<i>Cr</i>	0.000	<i>Cr</i>	0.000
<i>Ni</i>	0.000	<i>Ni</i>	0.000	<i>Ni</i>	0.000
<i>Total</i>	20.619	<i>Total</i>	20.383	<i>Total</i>	20.525

Table 7 Microprobe Analysis of Hornblende for Selected Specimens

<i>Ink8 p1 hb edge</i>		<i>Ink8 p1 hb</i>		<i>Ink4 p1 hbl</i>		<i>Ink13 p4 hb2</i>	
<i>Oxide</i>	<i>Weight %</i>	<i>Oxide</i>	<i>Weight %</i>	<i>Oxide</i>	<i>Weight %</i>	<i>Oxide</i>	<i>Weight %</i>
<i>SiO₂</i>	42.80	<i>SiO₂</i>	43.45	<i>SiO₂</i>	43.25	<i>SiO₂</i>	42.70
<i>TiO₂</i>	2.01	<i>TiO₂</i>	1.45	<i>TiO₂</i>	2.84	<i>TiO₂</i>	1.09
<i>Al₂O₃</i>	10.70	<i>Al₂O₃</i>	11.85	<i>Al₂O₃</i>	11.68	<i>Al₂O₃</i>	10.10
<i>Fe₂O₃</i>	0.00	<i>Fe₂O₃</i>	0.00	<i>Fe₂O₃</i>	0.00	<i>Fe₂O₃</i>	0.00
<i>FeO</i>	20.10	<i>FeO</i>	20.10	<i>FeO</i>	13.30	<i>FeO</i>	20.50
<i>MnO</i>	0.50	<i>MnO</i>	0.45	<i>MnO</i>	0.15	<i>MnO</i>	0.45
<i>MgO</i>	8.01	<i>MgO</i>	8.40	<i>MgO</i>	13.00	<i>MgO</i>	8.06
<i>CaO</i>	11.50	<i>CaO</i>	11.50	<i>CaO</i>	11.70	<i>CaO</i>	12.90
<i>Na₂O</i>	0.93	<i>Na₂O</i>	0.75	<i>Na₂O</i>	2.46	<i>Na₂O</i>	0.53
<i>K₂O</i>	1.73	<i>K₂O</i>	1.60	<i>K₂O</i>	0.48	<i>K₂O</i>	1.22
<i>Cl</i>	0.05	<i>Cl</i>	0.05	<i>Cl</i>	0.02	<i>Cl</i>	0.09
<i>P₂O₅</i>	0.00	<i>P₂O₅</i>	0.06	<i>P₂O₅</i>	0.00	<i>P₂O₅</i>	0.05
<i>Cr₂O₃</i>	0.00	<i>Cr₂O₃</i>	0.00	<i>Cr₂O₃</i>	0.03	<i>Cr₂O₃</i>	0.00
<i>NiO</i>	0.00	<i>NiO</i>	0.00	<i>NiO</i>	0.00	<i>NiO</i>	0.00
<i>Total</i>	98.33	<i>Total</i>	99.66	<i>Total</i>	98.91	<i>Total</i>	97.69
<i>No of Oxygens 23</i>		<i>No of Oxygens 23</i>		<i>No of Oxygens 23</i>		<i>No of Oxygens 23</i>	
<i>Si</i>	6.517	<i>Si</i>	6.497	<i>Si</i>	6.325	<i>Si</i>	6.566
<i>Ti</i>	0.230	<i>Ti</i>	0.164	<i>Ti</i>	0.312	<i>Ti</i>	0.126
<i>Al</i>	1.920	<i>Al</i>	2.088	<i>Al</i>	2.012	<i>Al</i>	1.830
<i>Fe³⁺</i>	0.000	<i>Fe³⁺</i>	0.000	<i>Fe³⁺</i>	0.000	<i>Fe³⁺</i>	0.000
<i>Fe²⁺</i>	2.559	<i>Fe²⁺</i>	2.513	<i>Fe²⁺</i>	1.626	<i>Fe²⁺</i>	2.636
<i>Mn</i>	0.064	<i>Mn</i>	0.056	<i>Mn</i>	0.018	<i>Mn</i>	0.059
<i>Mg</i>	1.815	<i>Mg</i>	1.872	<i>Mg</i>	2.834	<i>Mg</i>	1.848
<i>Ca</i>	1.876	<i>Ca</i>	1.842	<i>Ca</i>	1.833	<i>Ca</i>	2.125
<i>Na</i>	0.275	<i>Na</i>	0.217	<i>Na</i>	0.698	<i>Na</i>	0.158
<i>K</i>	0.335	<i>K</i>	0.306	<i>K</i>	0.090	<i>K</i>	0.239
<i>Cl</i>	0.006	<i>Cl</i>	0.006	<i>Cl</i>	0.003	<i>Cl</i>	0.011
<i>Total</i>	15.597	<i>Total</i>	15.561	<i>Total</i>	15.751	<i>Total</i>	15.598
<i>Fe No*</i>	59.060	<i>Fe No*</i>	57.850	<i>Fe No*</i>	36.720	<i>Fe No*</i>	59.320
<i>Mg No*</i>	40.940	<i>Mg No*</i>	42.150	<i>Mg No*</i>	63.280	<i>Mg No*</i>	40.680
<i>Total</i>	100.000	<i>Total</i>	100.000	<i>Total</i>	100.000	<i>Total</i>	100.000
<i>Fe=(Fe³⁺ + Fe²⁺ + Mn)</i>							

Table 8 Microprobe Analysis of Vesuvianite, Wollastonite, Titanite and Chlorite for Selected Specimens

<i>Inkl2 ves.incl in gl</i>		<i>Inkl10 wo</i>		<i>Inkl3sphene</i>		<i>Inkl7 sphene</i>		<i>Inkl7 chlorite</i>	
<i>Oxide</i>	<i>Weight %</i>								
<i>SiO₂</i>	36.40	<i>SiO₂</i>	51.40	<i>SiO₂</i>	30.60	<i>SiO₂</i>	30.50	<i>SiO₂</i>	28.80
<i>TiO₂</i>	3.16	<i>TiO₂</i>	0.10	<i>TiO₂</i>	31.80	<i>TiO₂</i>	30.60	<i>TiO₂</i>	0.00
<i>Al₂O₃</i>	14.20	<i>Al₂O₃</i>	1.10	<i>Al₂O₃</i>	1.90	<i>Al₂O₃</i>	2.66	<i>Al₂O₃</i>	18.40
<i>Fe₂O₃</i>	0.00								
<i>FeO</i>	4.00	<i>FeO</i>	0.00	<i>FeO</i>	1.10	<i>FeO</i>	0.70	<i>FeO</i>	21.20
<i>CaO</i>	36.40	<i>CaO</i>	48.80	<i>CaO</i>	27.80	<i>CaO</i>	28.40	<i>CaO</i>	0.29
<i>MgO</i>	2.50	<i>MgO</i>	0.07	<i>MgO</i>	0.00	<i>MgO</i>	0.00	<i>MgO</i>	20.50
<i>MnO</i>	0.02	<i>MnO</i>	0.21	<i>MnO</i>	0.01	<i>MnO</i>	0.00	<i>MnO</i>	0.77
<i>Na₂O</i>	0.01	<i>Na₂O</i>	0.00	<i>Na₂O</i>	0.25	<i>Na₂O</i>	0.00	<i>Na₂O</i>	0.35
<i>K₂O</i>	0.26	<i>K₂O</i>	0.00	<i>K₂O</i>	0.01	<i>K₂O</i>	0.00	<i>K₂O</i>	0.02
<i>Cl</i>	0.38	<i>Cl</i>	0.00	<i>Cl</i>	0.00	<i>Cl</i>	0.01	<i>Cl</i>	0.04
<i>P₂O₅</i>	0.14	<i>P₂O₅</i>	0.00	<i>P₂O₅</i>	0.30	<i>P₂O₅</i>	0.19	<i>P₂O₅</i>	0.00
<i>Cr₂O₃</i>	0.00								
<i>NiO</i>	0.00	<i>NiO</i>	0.00	<i>NiO</i>	0.28	<i>NiO</i>	0.00	<i>NiO</i>	0.00
<i>Total</i>	97.47	<i>Total</i>	101.68	<i>Total</i>	94.05	<i>Total</i>	93.06	<i>Total</i>	90.37
<i>No of Oxygens 32</i>		<i>No of Oxygens 32</i>		<i>No of Oxygens 5</i>		<i>No of Oxygens 5</i>		<i>No of Oxygens 24</i>	
<i>Si</i>	5.856	<i>Si</i>	1.953	<i>Si</i>	1.050	<i>Si</i>	1.279	<i>Si</i>	4.949
<i>Ti</i>	0.381	<i>Ti</i>	0.003	<i>Ti</i>	0.852	<i>Ti</i>	0.965	<i>Ti</i>	0.000
<i>Al</i>	2.693	<i>Al</i>	0.060	<i>Al</i>	0.077	<i>Al</i>	0.131	<i>Al</i>	3.727
<i>Fe³⁺</i>	0.000								
<i>Fe²⁺</i>	0.537	<i>Fe²⁺</i>	0.000	<i>Fe²⁺</i>	0.037	<i>Fe²⁺</i>	0.024	<i>Fe²⁺</i>	2.000
<i>Ca</i>	6.277	<i>Ca</i>	1.988	<i>Ca</i>	1.014	<i>Ca</i>	1.274	<i>Ca</i>	0.052
<i>Mg</i>	0.598	<i>Mg</i>	0.004	<i>Mg</i>	0.000	<i>Mg</i>	0.000	<i>Mg</i>	5.243
<i>Mn</i>	0.001	<i>Mn</i>	0.007	<i>Mn</i>	0.000	<i>Mn</i>	0.000	<i>Mn</i>	0.111
<i>Na</i>	0.001	<i>Na</i>	0.000	<i>Na</i>	0.012	<i>Na</i>	0.000	<i>Na</i>	0.112
<i>K</i>	0.052	<i>K</i>	0.000	<i>K</i>	0.000	<i>K</i>	0.000	<i>K</i>	0.003
<i>Cl</i>	0.101	<i>Cl</i>	0.000	<i>Cl</i>	0.000	<i>Cl</i>	0.000	<i>Cl</i>	0.011
<i>P</i>	0.019	<i>P</i>	0.000	<i>P</i>	0.007	<i>P</i>	0.007	<i>P</i>	0.000
<i>Cr</i>	0.000								
<i>Ni</i>	0.000	<i>Ni</i>	0.000	<i>Ni</i>	0.005	<i>Ni</i>	0.000	<i>Ni</i>	0.000
<i>Total</i>	16.516	<i>Total</i>	4.015	<i>Total</i>	3.054	<i>Total</i>	3.680	<i>Total</i>	16.208

Appendix 2
Description of Thin Sections

Ink2

Calcsilicate rock with garnets

The groundmass of the specimen consists of with wollastonite grains, which show multiple twinning. A small calcite vein intersects the wollastonite ground mass.

Subhedral garnet crystals are included in the groundmass. These garnets contain various inclusions of the ground mass minerals epidote, diopside, sphene and wollastonite. There are inclusions of zircon in some of the garnets. These garnets show distinct core-rim, where inclusions show zoning in the grain size. Larger inclusions are on the edge, becoming much finer grained towards the centre of the garnet grains. The outer rims show lots of acicular wollastonite crystals with random orientation. In the core of the garnets there is no wollastonite. The core contains mainly diopside inclusions. Vesuvianite grains are mainly at the rim-core boundary.

Although garnet crystals are zoned in relation to inclusions size, there is no zoning in chemical content. All garnets are grossularite - andradite.

Ink10

Calcsilicate rock with garnet, wollastonite, calcite and diopside

The thin section consists of wollastonite and euhedral to subhedral garnet crystals and minor diopside.

Wollastonite grains in the matrix are mainly elongated, and define a strong foliation that wraps around garnet grains. These wollastonite grains show multiple twinning. Diopside grains also come as inclusions in the matrix.

Garnets are grossularite - andradite. Garnets are large and irregular, and have abundant inclusions, mainly diopside, sphene, calcite, epidote and wollastonite.

These inclusions appear to be randomly oriented. Besides the strong foliation, wollastonite grains have been recrystallised to very fine aggregates along very thin mylonite zones.

Ink12

Layered calcsilicate rock

This specimen is a thinly laminated and contains two types of layers.

Granite- tonalite layers: these layers are 0.5 to 2 cm thick granitic veins. Their average content is 50% quartz and 40% plagioclase, minor titanite, biotite, clinopyroxene and epidote. Evident is feldspar alteration to sericite. Epidote crystals show anomalous blue interference colours, probably clinzoisite. This vein contains numerous inclusions of pyrite and pyrrhotite, approximately 0.5-1% (very red)? Magnetite occurs as inclusions in sphene crystals.

Mafic layers: 1-1.5 cm thick. These layers contain approximately 25% clinopyroxene, 60% plagioclase, 10% quartz and 2% titanite. Large clinopyroxene crystals show well-developed cleavage. In plane polarised light they show green to pale green colour. They also contain inclusions of sphene.

Ink12a

Layered calcsilicate rock, very similar to rock from Ink12.

The specimen shows a few different layers.

The two granitic layers vary in thickness from 0.3 to 0.7 cm. These two layers are separated with a thin (0.3 cm) more mafic layer mainly with plagioclase and pyroxene. The plagioclase grains are partially altered, possibly to sericite. In plane polarised light they are light green to very light brown colour.

A layer of massive garnet is 0.8 to 1cm thick. The garnets are euhedral to anhedral. Epidote occurs interstitial to garnet, and appears to have replaced

garnet along irregular fractures and atoll structures. Thin veins of epidote occur throughout the rock.

Ink13

Layered calcsilicate rock

This rock is layered with some layers being of granitic (tonalitic) composition. Other are calcsilicate layers consisting of quartz, epidote-clinozoisite, garnet, titanite and altered plagioclase.

Granitic layers are 0.2 to 0.5 cm thick, mainly consisting of quartz, feldspar, plagioclase, diopside, hornblende, magnetite and sphene. In plane polarised light diopside shows very pale green colour. These diopside grains also contain small titanite inclusions.

Ink8

Calcsilicate with granitic vein

This specimen consists of a finer grained poikiloblastic part with plagioclase, diopside, minor green and brown hornblende and opaques.

Irregular patches or veins of slightly coarser rock consist of plagioclase, quartz and diopside, and appear to be granitic (tonalitic) in composition and texture. Alteration of plagioclase to sericite and saussurite occurs in parts of the thin section.

Throughout the specimen there are scattered small cubic crystals that show dark red colour in plane polarised light, possible pyrite crystals.

This rock is possible calcsilicate, but a possibility that it is a rock of a basaltic origin cannot be discounted.

Ink7

Amphibolite

This specimen is mostly medium to coarse-grained rock with:

20% amphibole,

50% altered plagioclase,

15% chlorite,

2% quartz,

5% opaque minerals,

2% titanite.

Amphiboles come as elongated crystals that show twinning. In plane polarised light they show green to brown colour. These elongated amphibole grains define strong foliation trend. The retrograde chlorite is also parallel to the foliation, has patches of very fine-grained sphene, and may have replaced biotite.

Ink6

Leuco Granite

This specimen has a medium grained igneous texture with minor hornblende crystals, which vary in size from 0.5 to 3 mm. Composition is:

40% quartz

25% plagioclase

30% k-feldspar, showing microcline and perthite

2% biotite

0.5% hornblende

Magnetite and sphene are accessory minerals.

Biotite comes in elongated crystals and show very yellow to rusty yellow colour in plane polarised light. Sometimes, biotite crystals fill in the spaces between feldspars. Generally this is a fresh rock, with little alteration. Quartz in undulose and has been recrystallised to finer grained matrix which include amoeboid grains that define foliation.

Ink11

Layered calc-silicate rock

This is very thinly laminated rock with medium grained layers of mainly feldspar and quartz. These layers vary in size from 0.1 to 0.5 cm. In some cases intergrowth of quartz and plagioclase form myrmekitic texture. Fine-grained sphene is abundant. Some thin layers consist mainly of quartz and plagioclase and are tonalitic in composition and texture. Feldspars from the layers have altered to epidote-clinozoisite. Minor opaques are present.

Mafic layers are 0.8 to 1 cm thick. These layers consist of quartz, plagioclase and clinopyroxenes, which define a strong foliation. On the edges pyroxenes have altered to chlorite.

Ink4

Andesite or basalt

This is a medium grained rock and shows no foliation. It contains:

30% plagioclase

5% quartz

60% hornblende

10% apatite

5% opaques

0.5% sphene

In plane polarised light large hornblende crystals show pleochroism from green to brown. A few of these crystals show the characteristic shape and two cleavages at 120°.

Plagioclase grains are laths to short prisms, and show zoning where the core is more Ca rich. Some of the plagioclase crystals have small inclusions of hornblende. Feldspars are not clear and they are altered to chlorite, clays and epidote.

The overall texture is subophitic with quartz interstitial to hornblende and plagioclase.

Ink14

Basalt dyke

This rock consists of plagioclase laths (60%), clinopyroxene (partly replaced by chlorite and actinolite) and 5% interstitial quartz. Plagioclase is partly altered to sericite, chlorite and calcite.

Abundant magnetite crystals are evenly dispersed throughout the specimen (7% magnetite).

Damien Fosters thin sections:

HH4

Calcsilicate layered rock

The specimen represents very foliated and layered rock. It contains very thin layers consisting mainly of quartz and plagioclase, 0.5 to 4 mm thick, alternating with clinopyroxene and plagioclase layers, 3 to 7 mm thick. The clinopyroxene appear to be variable in composition, as it is deep green in some layers and light green in others. Accessory magnetite is present.

The foliation is defined by alignment of elongated plagioclase and clinopyroxene.

HH7

Paragneiss

This specimen is a calcsilicate rock with a vein of pegmatitic monzogranite.

The pegmatitic vein is approximately 1.5 to 2 cm thick. It consists mainly of quartz, plagioclase and k-feldspar. The feldspars are strained (undulose) porphyroblasts, surrounded by recrystallised quartz that is granular to amoeboid in texture. Also present are very thin discontinuous zones of mylonitized quartz of quite fine grain size.

The calcsilicate layer is 0.3 to 1 cm thick. It consists mainly of clinopyroxene and plagioclase, with several large hornblende grains and accessory sphene and opaques. In plane polarised light large and elongated hornblende grains show green-brown pleochroism. The texture of the calcsilicate rock is essentially polyzonal with a weak foliation defined by slightly elongated clinopyroxene and plagioclase.

On the contact between the pegmatitic vein and calcsilicate are concentrated diamond shaped sphene crystals.

HHA9

Tonalitic vein in paragneiss

This specimen is similar to the rock from the thin section HH7.

The tonalitic vein contains approximately:

35% quartz

60% plagioclase

5% k-feldspars

There is a good example of an allanite crystal with distinctive zoning and radiating expansion cracks.

Medium to coarse grained more mafic layers contain clusters of clinopyroxene surrounded by hornblende. These are veined by the tonalite where the hornblende being likely in reaction rims. The original host was possibly a calcsilicate.

H3

Calcsilicate rock

The rock consists of wollastonite, diopside, garnet, quartz, scapolite, tremolite and accessory titanite. A strong foliation is defined by alignment of wollastonite and diopside, but one portion of the slide shows coarser grained scapolite and garnet.

H2

Layered calcsilicate rock

This specimen is a thinly laminated rock. Massive garnet layers are 0.5 to 1 cm thick. The garnets contain abundant diopside inclusions and some quartz inclusions.

The layers that consist of variable amounts of diopside, wollastonite, calcite, garnet, scapolite and accessory sphene, are 0.1 to 0.5 cm thick. A strong foliation is defined by the lamination and alignment of elongated wollastonite, calcite and diopside. Cloudy grains may be altered plagioclase.

HHA12

Endoskarn development in granodiorite

This is medium to fine grained rock with:

20% quartz

60% plagioclase

10% k-feldspar

10% hornblende and pyroxenes

2% sphene

In some cases intergrowth of quartz and plagioclase form myrmekitic texture.

Some of the hornblende crystals have been replaced by diopside, sphene and opaques. The rock may be an endoskarn.

HHA6

Calcsilicate rock with pegmatitic veins

The rock consists mainly of thin layers of varying proportions of pyroxene, garnet, sphene and opaque minerals. The primary foliation, which was a layered calcsilicate foliation, is lost.

A few very thin, 1 – 2 mm, pegmatitic veins run parallel to the calcitic layers. These veins mainly consist of k-feldspars, pyroxene, plagioclase and quartz.

HHA2

Pegmatitic vein

This vein consists mainly of quartz (35%), k-feldspar (50%), plagioclase (10%) pyroxene, epidote and sphene (5%). Pyroxene comes as large crystals (1-3mm) and has inclusions of sphene. Quartz has been recrystallised with the development of mylonitic texture.

HHA7

Calcsilicate rock with pegmatitic vein

The pegmatitic vein consists of quartz (30%), k-feldspar (50%) and plagioclase (15%). Evident is alteration of feldspars to prehnite. Prehnite come in a form of radiating crystals. Subhedral garnet grains come as inclusions in the pegmatitic vein. A fibrous radiating mineral may be clinozoisite.

HH6.2.a

Calcsilicate rock with granitic vein

The granitic vein is approximately 1 - 1.5 cm thick and consists mainly of quartz, plagioclase, minor hornblende and sphene. The grain size of quartz and feldspars vary from coarse grained to fine grained layers. The coarse grained layers have large deep green hornblende grains. These coarse grained layers gradually become finer grained, with numerous small grains of sphene, pyroxene and hornblende. In quartz rich layers, the plagioclase grains have abundant quartz inclusions.

Other layers consist of epidote, garnet and quartz. A foliation is shown by elongate, recrystallised quartz in some layers.

HH6.2.b

Layered calcsilicate rock with granitic veins

This is similar rock to the rock in HH6.2.a where granitic veins are mainly coarse grained, with large amphibole grains parallel to the layers. Pyroxene is present in some layers, and there is no garnet in this specimen.

HH A1

Massive calcsilicate rock

The specimen consists of massive garnet with inclusions of wollastonite calcite and minor vesuvianite. Wollastonite comes in a form of bladed crystals. The garnets vary in grain size. The matrix consists of wollastonite, pyroxene and calcite.

HH A8

Calcsilicate rock

The specimen consists of garnet, plagioclase, pyroxene and sphene. Primary layering can be recognised. In plane polarised light pyroxenes show green colour. The specimen shows a well-developed polygonal texture.

HH3

Intermediate dyke

This specimen is mostly medium grained rock with:
40% amphibole, as brown prismatic grains,
45% plagioclase, cloudy and altered to epidote,
10% chlorite, as an alteration mineral.
2% quartz,
3% opaque minerals,

Amphiboles come as elongated crystals that show twinning. The specimen shows no foliation.

HI

Layered calcsilicate rock

This specimen presents layered rock with varying proportion of clinopyroxene, quartz and plagioclase layers (0.2 - 1.2 cm) and alternating layers of granitic composition (0.1 - 0.4 cm). These granitic layers consist mainly of quartz, plagioclase and pyroxene. Also is present accessory sphene. A strong foliation is preserved.

HH5

Granite

This is medium grained rock with:

40% quartz

40% plagioclase

10% k-feldspar

2% hornblende

2% pyroxene

1% biotite

Magnetite and sphene are accessory minerals.

HH1 and HH2

Granite

This is a medium to coarse-grained rock. In composition is similar to the rock from thin section HH5 but with a much higher proportion of k-feldspar. There is no hornblende or pyroxene present. Feldspars have been altered to sericite.

HH6.1.b (1)

Calcsilicate rock with granitic vein

Layers rich in garnet, vary in thickness from 0.3 - 2 cm. These layers also contain quartz, plagioclase and diopside.

A few thin (0.5 – 1 mm) granitic veins crosscut these garnet layers.

The granitic veins run parallel to the calcsilicate layers, and vary in thickness from 0.3 to 0.5 cm. These veins consist mainly of quartz and plagioclase. Sphene comes as small inclusions in these granitic veins.

HH6.1.b (2)

Calcsilicate rock with granitic vein

This is similar rock as in thin section HH6.1.b (2). Contain layers of garnets, plagioclase and quartz. The granitic veins consist mainly of quartz and plagioclase and are parallel to garnet, plagioclase and quartz layers.

Appendix 3

List of Thin Sections With Catalogue Number

Thin Section Name	JCU Catalogue Number
Ink2	63546
Ink10	63547
Ink12	63548
Ink12a	63549
Ink13	63550
Ink8	63551
Ink7	63552
Ink6	63553
Ink11	63554
Ink4	63555
Ink14	63556

D. Fosters Thin Sections

HH4	63557
HH7	63558
HHA9	63559
H3	63560
H2	63561
HHA12	63562
HHA6	63563
HHA2	63564
HHA7	63565
HH6.2.a	63566
HH6.2.b	63567
HHA1	63568
HHA8	63569
HH3	63570
H1	63571
HH5	63572
HH1	63573
HH2	63574
HH6.1.b (1)	63575
HH6.1.b (2)	63576